Polarization in inclusive reactions*

Frank E. Paige†
Department of Physics, B-019, University of California, San Diego, La Jolla, California 92093

D. P. Sidhu
Brookhaven National Laboratory, Upton, New York 11973

(Received 2 July 1976)

We estimate the contribution of Regge-cut graphs to the single-polarization measurements such as the polarization of the outgoing particle P_c, the polarized-beam asymmetry Σ_a, and the polarized-target asymmetry Σ_b for inclusive reactions in the triple-Regge region. We find that in the energy region where these cut graphs may be important relative to other contributions, all the single-polarization observables are small, roughly $\lesssim 5\%$. Comparisons are made with the available data on these spin observables. We also discuss the implications of those results for triple-Regge phenomenology.

I. INTRODUCTION

Data are starting to become available on polarization phenomena in inclusive reactions. In this paper we study the description of such data in the triple-Regge kinematic region. The unpolarized cross section in this region is well described by diagonal triple-Regge pole graphs, those in which the two Reggeons with nonzero momentum transfer are identical.[1] It turns out that polarizations arise only from nondiagonal pole graphs or from Regge-cut graphs.[2] Thus, the study of polarizations should provide a more detailed test of the Regge description of inclusive reactions.

Consider the one-particle inclusive reaction

$$a+b\to c+X, \tag{1.1}$$

where X denotes anything (see Fig. 1). In the triple-Regge kinematic region $t=(p_a-p_c)^2$ is small, while $s=(p_a+p_b)^2$, $M^2=(p_a+p_b-p_c)^2$, and s/M^2 are all large. Besides the unpolarized cross section three single-polarization parameters can be measured[2-7]: the polarization P_c of the observed particle c and the asymmetry parameters Σ_a and Σ_b for polarizations of the initial particles a and b. More complicated double- and triple-spin correlations can also be investigated, but we do not consider them here. By a trivial generalization of Mueller's optical theorem[8,3] all observables can be expressed as discontinuities of amplitudes for $a+b+\bar{c}\to a'+b'+\bar{c}'$ with appropriate helicities.

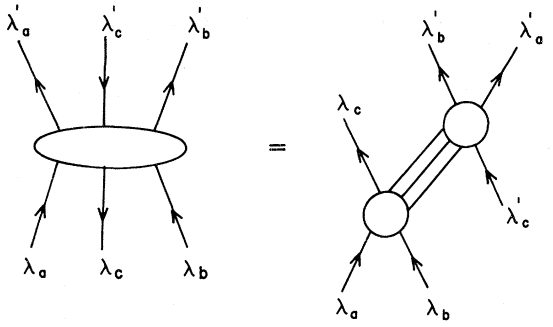

FIG. 1. The amplitude $A_{\lambda_a'\lambda_b'\lambda_c';\lambda_a\lambda_b\lambda_c}$.

The simplest graphs applicable to inclusive reactions in the triple-Regge region are the triple-Regge pole graphs[9,10] shown in Fig. 2. All of the helicity dependence of such graphs obviously comes from the external two-body Regge residues, which are presumably known. Thus the contribution of such a graph to any spin observable can be calculated once the triple-Regge vertex is known. In particular, the asymmetry parameter Σ_b vanishes for any such graph since it turns out to involve a helicity flip at the $\alpha_3 b\bar{b}$ vertex, which has zero momentum transfer.[3]

For P_c and Σ_a not much can be said at present about the triple-Regge pole graphs.[2] Fits to the unpolarized cross sections[1] have determined only the triple-Regge vertices with $\alpha_1=\alpha_2$, and these do not contribute to P_c or Σ_a. While the graphs with $\alpha_1\neq\alpha_2$ do contribute to the unpolarized cross section, it is not possible to separate them in practice. Thus the nondiagonal vertices must be determined by fitting polarization data as a function of s and M^2. The graphs which are expected to contribute to several reactions of interest are given below. For $pp\to\Lambda X$ there may be a term which is independent of s at fixed $x=1-M^2/s$, but in most other cases P_c and Σ_a should decrease like $(s)^{-1/2}$ at fixed x. Thus, experiments at relatively low energies are appropriate.

The Regge-cut graphs which contribute to inclusive reactions in the triple-Regge region could be almost arbitrarily complicated. However, we believe that Pomeron interactions are weak, so

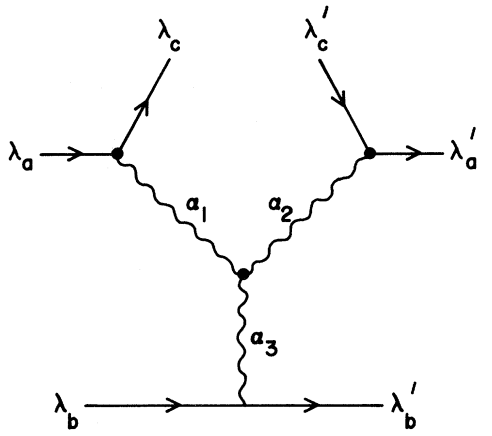

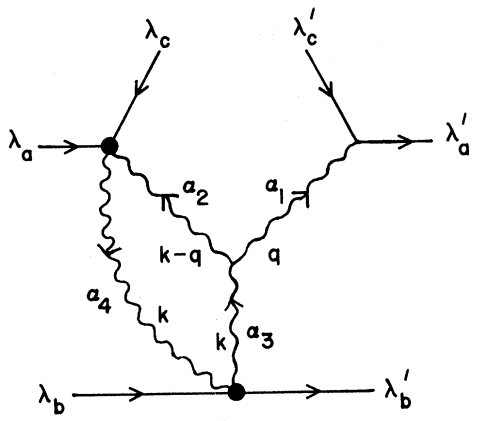

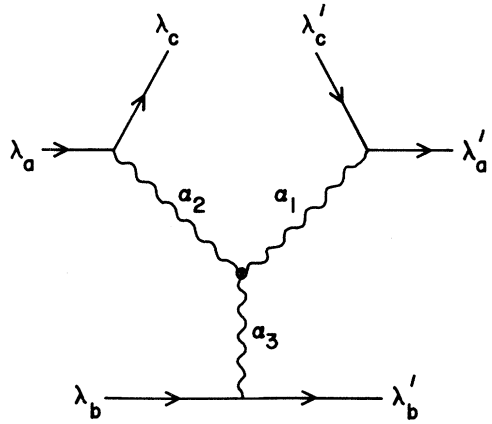

FIG. 2. The triple-Regge graphs $(\alpha_1, \alpha_2, \alpha_3)$.

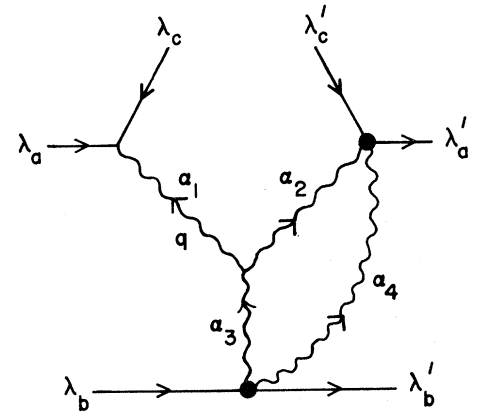

FIG. 3. The Regge-cut graphs $(\alpha_1, \alpha_2, \alpha_3, \alpha_4)$.

that it makes sense to keep only those graphs with a single triple-Regge vertex; see Fig. 3. This is similar to the approximation generally made in absorption-model calculations for two-body reactions.[11,12] While such an approximation is too crude to describe the physical Pomeron correctly, it should provide a reasonable estimate of the effects of Pomeron cuts on meson-exchange graphs, and this is all that is required.

The contribution of the graphs shown in Fig. 3 to the unpolarized cross section has been studied previously by us.[13] Here we study their contributions to the polarization parameters P_c, Σ_a, and Σ_b. For P_c and Σ_a we concentrate on graphs in which α_3 and α_4 are both Pomerons, since such graphs give polarizations which are independent of s at fixed x within logarithms. Our main result is that the polarization arising from such graphs is only a few percent in all cases. Graphs in which α_3 or α_4 is a meson could also be calculated, but we believe that they are not very important even at moderate energy. In any event their contributions would be difficult to isolate experimentally since their energy dependence is similar to that of allowed pole graphs.

For Σ_b we need a helicity flip on the $b\bar{b}$ side of the graph, so we must consider graphs in which either α_3 or α_4 is a meson. These graphs behave like $(s)^{-1/2}$.

The plan of the rest of this paper is as follows: In Sec. II general formulas for the polarization parameters in terms of the Mueller amplitude are given and the contributions of triple-Regge-pole graphs are studied. Several specific reactions are discussed. In Secs. III Regge-cut graphs of the sort shown in Fig. 3 are analyzed. In Sec. IV specific models for the Reggeon vertices are introduced. Numerical results are pre-

sented for several specific reactions and compared with experimental data. In Sec. V some general conclusions are drawn. There are three Appendixes containing technical details.

II. TRIPLE-REGGE POLE GRAPHS

A. Kinematics

Consider the inclusive reaction

$$a+b\to c+X, \tag{2.1}$$

where particles a, b, and c have spins s_a, s_b, and s_c, and where X denotes anything. The independent kinematic variable can be taken to be

$$\begin{aligned} s&=(p_a+p_b)^2,\\ M^2&=(p_a+p_b-p_c)^2,\\ t&=(p_a-p_c)^2. \end{aligned} \tag{2.2}$$

It is also convenient to introduce

$$x=1-\frac{M^2}{s}. \tag{2.3}$$

Then the triple-Regge kinematic region[9] is that which s, M^2, and s/M^2 are all large while t is small. (The particles between which the momentum transfer is small shall always be labeled a and c.)

According to Mueller's generalized optical theorem[8] all of the observables for this reaction can be expressed in terms of amplitudes $A_{\lambda_a'\lambda_b'\lambda_c';\lambda_a\lambda_b\lambda_c}$, each of which is the M^2 discontinuity of an S-matrix element for $a+b+\bar{c}\to a'+b'+\bar{c}'$ with a $-i\epsilon$ prescription for the outgoing energy $s'=(p_a'+p_b')^2$.[14,15] See Fig. 1. The helicity labels λ_i are the s-channel helicities for the reaction $a+b\to c+X$. In particular let σ_1 be the one-particle unpolarized inclusive cross section, P_c be the polarization of c, and Σ_a and Σ_b by the asymmetry parameters for polarizations of a and b. By parity invariance these polarizations should be normal to the scattering plane. Then if the polarized particles have spin $\frac{1}{2}$,[2-7]

$$\sigma_1=s\frac{d\sigma}{dt\,dM^2}=\frac{1}{(2s_a+1)(2s_b+1)}\sum_{\lambda_a\lambda_b\lambda_c}A_{\lambda_a\lambda_b\lambda_c;\lambda_a\lambda_b\lambda_c}, \tag{2.4}$$

$$P_c\sigma_1=\frac{-i}{(2s_a+1)(2s_b+1)}\times\sum_{\lambda_a\lambda_b}(A_{\lambda_a\lambda_b+;\lambda_a\lambda_b-}-A_{\lambda_a\lambda_b-;\lambda_a\lambda_b+}), \tag{2.5}$$

$$\Sigma_a\sigma_1=\frac{i}{2(2s_b+1)}\times\sum_{\lambda_b\lambda_c}(A_{+\lambda_b\lambda_c;-\lambda_b\lambda_c}-A_{-\lambda_b\lambda_c;+\lambda_b\lambda_c}), \tag{2.6}$$

$$\Sigma_b\sigma_1=\frac{i}{2(2s_a+1)}\times\sum_{\lambda_a\lambda_c}(A_{\lambda_a+\lambda_c;\lambda_a-\lambda_c}-A_{\lambda_a-\lambda_c;\lambda_a+\lambda_c}). \tag{2.7}$$

These formulas are derived in Appendix A.

B. Amplitudes and observables

The triple-Regge pole graphs, Fig. 2, have been discussed extensively in the literature. In what follows such graphs shall always be labeled by their Regge trajectories in the order $(\alpha_1\alpha_2\alpha_3)$. The Mueller amplitude for these graphs is[3]

$$A_{\lambda_a'\lambda_b'\lambda_c';\lambda_a\lambda_b\lambda_c}=\frac{1}{16\pi s}[\beta^1_{\lambda_c'\lambda_a'}(t)\beta^2_{\lambda_c\lambda_a}(t)\xi_1^*(t)\xi_2(t)+\beta^2_{\lambda_c'\lambda_a'}(t)\beta^1_{\lambda_c\lambda_a}(t)\xi_2^*(t)\xi_1(t)]\times g_{12,3}(t,t,0)\beta^3_{\lambda_b'\lambda_b}(0)\left(\frac{s}{M^2}\right)^{\alpha_1(t)+\alpha_2(t)}(M^2)^{\alpha_3(0)}, \tag{2.8}$$

where $\alpha_i(t)$ and $\beta^i_{\lambda\mu}(t)$ are the usual Regge trajectory functions and two-body residues, with s-channel helicities,

$$\xi_i(t)=\frac{e^{-i\pi\alpha_i(t)}+\tau_i}{-\sin\pi\alpha_i(t)} \tag{2.9}$$

are the signature factors, and $g_{12,3}(t,t,0)$ is the triple-Regge vertex. It should be noted that all helicity dependence in Eq. (2.8) comes from the Regge residues. For $\alpha_1=\alpha_2$ there is only one graph, and it is conventional not to include an extra factor of 2 such as would be obtained by setting $\alpha_1=\alpha_2$ in Eq. (2.8).

From Eq. (2.4) and Eq. (2.8) the unpolarized cross section is

$$\sigma_1=\frac{1}{16\pi s}\frac{1}{(2s_a+1)(2s_b+1)}\left(\sum_{\lambda_a\lambda_c}\beta^1_{\lambda_c\lambda_a}\beta^2_{\lambda_c\lambda_a}\right)2\,\mathrm{Re}(\xi_1^*\xi_2)g_{12,3}\left(\sum_{\lambda_b}\beta^3_{\lambda_b\lambda_b}\right)\left(\frac{s}{M^2}\right)^{\alpha_1+\alpha_2}(M^2)^{\alpha_3}. \tag{2.10}$$

Parity invariance implies that

$$\beta_{\lambda\mu}(t)=\eta(-1)^{\lambda-\mu}\beta_{-\lambda-\mu}(t), \tag{2.11}$$

where η is the naturality of the trajectory. From this it is trivial to show that σ_1 is zero if α_1 and α_2 have opposite naturality or if α_3 has unnatural parity.[2] Hence σ_1 can be written as the sum of a natural- and an unnatural-parity component:

$$\sigma_1=\sigma_1^N+\sigma_1^U. \tag{2.12}$$

It is also easy to see that $\mathrm{Re}(\xi_1^*\xi_2)$, and hence σ_1, vanish if α_1 and α_2 are exchange-degenerate and have opposite signature.

For spin-$\frac{1}{2}$ particles and natural-parity trajectories Eq. (2.10) simplifies to

$$\sigma_1^N=\frac{1}{16\pi s}(\beta^1_{++}\beta^2_{++}+\beta^1_{-+}\beta^2_{-+})\,2\,\mathrm{Re}(\xi_1^*\xi_2)\,g_{12,3}\beta^3_{++}\left(\frac{s}{M^2}\right)^{\alpha_1+\alpha_2}(M^2)^{\alpha_3}. \tag{2.13}$$

From Eq. (2.5) and Eq. (2.8) the polarization of particle c is given by

$$P_c\sigma_1=\frac{1}{16\pi s}\frac{1}{(2s_a+1)(2s_b+1)}\sum_{\lambda_a}(\beta^1_{+\lambda_a}\beta^2_{-\lambda_a}-\beta^1_{-\lambda_a}\beta^2_{+\lambda_a})\,2\,\mathrm{Im}(\xi_1^*\xi_2)\,g_{12,3}\left(\sum_{\lambda_b}\beta^3_{\lambda_b\lambda_b}\right)\left(\frac{s}{M^2}\right)^{\alpha_1+\alpha_2}(M^2)^{\alpha_3}. \tag{2.14}$$

As for the cross section, it is easy to show that P_c vanishes if α_1 and α_2 have opposite naturality or if α_3 has unnatural parity.[2] Hence P_c can be expressed as the sum of a natural- and an unnatural-parity component:

$$P_c\sigma_1=P_N\sigma_1^N+P_U\sigma_1^U. \tag{2.15}$$

It also follows from Eq. (2.14) that P_c vanishes if α_1 and α_2 are exchange degenerate and have the same signature, or if their residues are exchange degenerate. Finally, since the polarization arises from an interference between helicity-flip and nonflip amplitudes, both types of couplings are needed. These constraints strongly limit the set of triple-Regge graphs which can contribute to P_c.

For spin-$\frac{1}{2}$ particles and natural-parity trajectories Eq. (2.14) simplifies to

$$P_N\sigma_1^N=\frac{1}{16\pi s}(\beta^1_{++}\beta^2_{-+}-\beta^1_{-+}\beta^2_{++})2\,\mathrm{Im}(\xi_1^*\xi_2)\,g_{12,3}\beta^3_{++}\left(\frac{s}{M^2}\right)^{\alpha_1+\alpha_2}(M^2)^{\alpha_3}. \tag{2.16}$$

From Eq. (2.6) and Eq. (2.8) the asymmetry parameter for polarization of particle a is given by

$$\Sigma_a\sigma_1=-\frac{1}{16\pi s}\frac{1}{2(2s_b+1)}\sum_{\lambda_c}(\beta^1_{\lambda_c+}\beta^2_{\lambda_c-}-\beta^1_{\lambda_c-}\beta^2_{\lambda_c+})2\,\mathrm{Im}(\xi_1^*\xi_2)\,g_{12,3}\left(\sum_{\lambda_b}\beta^3_{\lambda_b\lambda_b}\right)\left(\frac{s}{M^2}\right)^{\alpha_1+\alpha_2}(M^2)^{\alpha_3}. \tag{2.17}$$

Comparison with Eq. (2.14) and Eq. (2.15) shows that

$$\Sigma_a\sigma_1=P_N\sigma_1^N-P_U\sigma_1^U. \tag{2.18}$$

Hence all of the comments about P_c also apply to Σ_a, although the two are not equal if there is unnatural-parity exchange.

Finally, from Eq. (2.7) and Eq. (2, 8) it follows that the asymmetry parameter Σ_b is proportional to $\beta^3_{+-}(0)$, which vanishes for a factorizable Regge pole.[3] Hence

$$\Sigma_b=0 \tag{2.19}$$

for any triple-Regge pole graph.

C. Specific reactions

A nonzero P_c or Σ_a can be obtained only from nondiagonal triple-Regge terms, those with $\alpha_1\neq\alpha_2$. Consider just the high-lying, natural-parity trajectories P, ω, f, ρ, A_2, K^*, and K^{**}. Then the only possible nondiagonal scaling terms are PfP and $K^*K^{**}P$. The PfP term should not contribute to P_c or Σ_a since both the P and the f have only nonflip couplings.[12,16] The $K^*K^{**}P$ vertex would vanish if the P were an SU(3) singlet,[2] but need not be zero otherwise. Its contribution to P_c and Σ_a will vanish if the K^* and K^{**} residues are exchange-degenerate.

The possible nonscaling terms are of two types, PMM and $M'M''M'''$, where M denotes any of the meson trajectories. Both types can contribute to P_c and Σ_a. Of course if the PMM coupling should be large, then the Regge-cut graphs considered in this paper would not be the dominant ones, but it need not be negligible.

The triple-Regge terms (and also the Regge-

TABLE I. Dominant graphs for P_c and Σ_a. We list what we expect to be the dominant graphs for σ_1 and for P_c or Σ_a in the triple-Regge region. Pole graphs are labeled by $\alpha_1\alpha_2\alpha_3$, cut graphs by $\alpha_1\alpha_2\alpha_3\alpha_4$. M refers to any of the ω, f, ρ, A_2 Regge poles. The behavior given is that of the invariant cross section σ_1, or $P_c\sigma_1$ or $\Sigma_a\sigma_1$ assuming that $\alpha_P=1$, $\alpha_M=\frac{1}{2}$, $\alpha_{K*}=\frac{1}{4}$ and ignoring logarithms. EXD stands for exchange-degenerate.

Reaction	Graph	Behavior	Comments
$pp\to(\Lambda,\Sigma^0)X$	K^*K^*P, $K^{**}K^{**}P$	$(1-x)^{1/2}(s)^0$	$P_c=0$; dominates σ_1
$p\pi\to(\Lambda,\Sigma^0)X$			
$pK\to(\Lambda,\Sigma^0)X$	$K^*K^{**}P$	$(1-x)^{1/2}(s)^0$	$P_c=0$ if residues EXD; absent if P is SU(3) singlet
	$K^*K^{**}M$	$(1-x)^0(s)^{-1/2}$	$P_c=0$ if residues EXD
	K^*K^*PP, $K^{**}K^{**}PP$	$(1-x)^{1/2}(s)^0$	P_c small
$\Sigma^-p\to(\Lambda,\Sigma^0)X$	$\rho\rho P$, A_2A_2P	$(1-x)^0(s)^0$	$P_c=0$; dominates σ_1
	$\rho A_2\omega$, ρA_2A_2	$(1-x)^{-1/2}(s)^{-1/2}$	$P_c=0$ if residues EXD
	$\rho\rho PP$, A_2A_2PP	$(1-x)^0(s)^0$	P_c small
$pp\to pX$	PPP	$(1-x)^{-1}(s)^0$	$P_c=0$; dominates σ_1 for $x\gtrsim0.9$
	MMP	$(1-x)^0(s)^0$	$P_c=0$; dominates σ_1 for $x\lesssim0.9$
	PfP	$(1-x)^{-1/2}(s)^0$	$P_c=0$ if $\beta^P_{-+}=\beta^f_{-+}=0$
	$P\rho\rho$, PA_2A_2	$(1-x)^{-1}(s)^{-1/2}$	$P_c\neq0$; nondiagonal triple-Regge vertex
	$\rho\omega A_2$, etc.	$(1-x)^{-1/2}(s)^{-1/2}$	$P_c\neq0$; nondiagonal triple-Regge vertex

cut terms) which could contribute to some typical reactions are listed in Table I. In the construction of this table it has been assumed that P, ω, and f couple only to nonflip, that ρ and A_2 couple mainly but not exclusively to flip, and that K^* and K^{**} couple both to flip and to nonflip amplitudes.[12,16]

III. REGGE-CUT GRAPHS

If Reggeon interactions are weak, as we believe, then the most important Regge-cut graphs should be those of the form shown in Fig. 3. Such graphs shall always be labeled by their Regge trajectories in the order $(\alpha_1,\alpha_2,\alpha_3,\alpha_4)$. The neglect of other Regge-cut graphs is an approximation similar to that made in the absorption model for two-body reactions[12]: The graph shown in Fig. 4(a) is kept while ones like that shown in Fig. 4(b) are discarded. Obviously this approximation is justified only if the relevant Pomeron-Reggeon-Reggeon vertices are small enough. Except for the triple-Pomeron vertex, which is small, these vertices have not been determined by the existing triple-Regge fits,[1] but some of them could be determined from measurements of polarizations. In particular the $P\rho\rho$ and PA_2A_2 graphs contribute to the polarization in $pp\to pX$.

This section is devoted to a general analysis of the graphs shown in Fig. 3. Numerical results for particular reactions are given in the following section.

A. Amplitudes and observables

By assumption the vertices of the graphs shown in Fig. 3 do not contain any additional Regge poles or other high-lying Regge singularities. Then the Mueller amplitude is

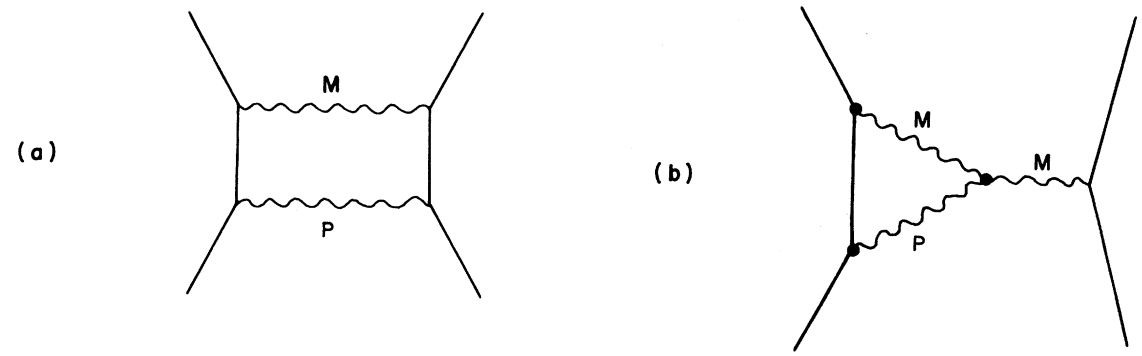

FIG. 4. Regge-cut graphs for two-body reactions.

$$A_{\lambda_a'\lambda_b'\lambda_c';\lambda_a\lambda_b\lambda_c} = \frac{1}{16\pi s}\int \frac{d^2k_\perp}{16\pi^2}\left[\beta^1_{\lambda_c'\lambda_a'}(t)N_{\alpha_2\lambda_c;\alpha_4\lambda_a}(t_2,t')N_{\alpha_3\lambda_b';\alpha_4\lambda_b}(t',t')i\xi_1^*(t)\xi_2(t_2)\xi_4(t')\right.$$
$$\left.+\beta^1_{\lambda_c\lambda_a}(t)N^*_{\alpha_2\lambda_c';\alpha_4\lambda_a'}(t_2,t')N_{\alpha_4\lambda_b';\alpha_3\lambda_b}(t',t')(-i)\xi_1(t)\xi_2^*(t_2)\xi_4^*(t')\right]g_{12,3}(t,t_2,t')$$
$$\times\left(\frac{s}{M^2}\right)^{\alpha_1(t_1)+\alpha_2(t_2)+\alpha_4(t')-1}(M^2)^{\alpha_3(t')+\alpha_4(t')-1}, \tag{3.1}$$

where here and in what follows

$$t=-q_\perp^2,\quad t'=-k_\perp^2,\quad t_2=-(q_\perp-k_\perp)^2. \tag{3.2}$$

This formula was derived in Ref. 17 and Ref. 18 and is rederived in Appendix B. The factors $N_{\alpha_2\lambda_c,\alpha_4\lambda_a}$ and $N_{\alpha_3\lambda_b'\alpha_4\lambda_b}$ are the usual Gribov Reggeon-particle vertices, which also appear in the formulas for Regge cuts in two-body reactions. (These vertices are real for spinless particles but not for particles with spin, as is shown below.) The factor $g_{12,3}(t,t_2,t')$ is the triple-Regge vertex, which for $t'=0$ is just that of the triple-Regge pole graph discussed in the previous section. Finally, the energy-dependent factors can be written as

$$\frac{1}{s}\left[\frac{1}{16\pi s}\left(\frac{s}{M^2}\right)^{\alpha_1+\alpha_2}(M^2)^{\alpha_3}\right](s)^{\alpha_4}, \tag{3.3}$$

where the factor in square brackets and the $(s)^{\alpha_4}$ correspond to the triple-Regge graph and the Regge pole α_4, respectively, and the $1/s$ is the usual Jacobian.

There is in general another pair of graphs having α_1 and α_2 interchanged. These two pairs are independent in the sense that they involve different Reggeon-particle vertices. If $\alpha_1=\alpha_2$, then there is only one triple-Regge graph and only one pair of Regge-cut graphs.

Equation (3.1) can be simplified by noting that if α_3 and α_4 have natural parity, as is assumed henceforth, then[18]

$$N_{\alpha_3\lambda_b',\alpha_4\lambda_b}=(-1)^{\lambda_b'-\lambda_b}N_{\alpha_4\lambda_b',\alpha_3\lambda_b}, \tag{3.4}$$

so that $N_{\alpha_3\lambda_b',\alpha_4\lambda_b}$ can be factored out of the square brackets.

The Regge-cut contribution to the unpolarized cross section σ_c is obtained by substituting Eq. (3.1) into Eq. (2.4):

$$\sigma_1=-\frac{1}{16\pi s}\frac{2}{(2s_a+1)(2s_b+1)}\int\frac{d^2k_\perp}{16\pi^2}\left[\sum_{\lambda_a\lambda_c}\beta^1_{\lambda_c\lambda_a}\mathrm{Im}(N_{\alpha_2\lambda_c,\alpha_4\lambda_a}\xi_1^*\xi_2\xi_4)\right]$$
$$\times(\Sigma_{\lambda_b}N_{\alpha_3\lambda_b,\alpha_4\lambda_b})g_{12,3}\left(\frac{s}{M^2}\right)^{\alpha_1+\alpha_2+\alpha_4-1}(M^2)^{\alpha_3+\alpha_4-1}. \tag{3.5}$$

This formula may appear strange because the imaginary part acts on $N_{\alpha_2\lambda_c,\alpha_4\lambda_a}$ as well as on $\xi_1^*\xi_2\xi_4$. As will be shown below, the Reggeon-particle vertex is not real for particles with spin, but its imaginary part comes only from phase factors associated with azimuthal rotations. These phase factors are such that $\mathrm{Im}(N)$ vanishes when integrated over all angles of $k_\perp$, so Eq. (3.5) is unchanged by the replacement

$$\mathrm{Im}(N_{\alpha_2\lambda_c,\alpha_4\lambda_a}\xi_1^*\xi_2\xi_4)\to\mathrm{Re}(N_{\alpha_2\lambda_c,\alpha_4\lambda_a})\mathrm{Im}(\xi_1^*\xi_2\xi_4). \tag{3.6}$$

It is then clear that the contribution of the cut graph subtracts from that of the pole graph if α_4 is a Pomeron.

If α_4 is a Pomeron, then the $(\alpha_1,\alpha_2,\alpha_3)$ and the $(\alpha_1,\alpha_2,\alpha_3,\alpha_4)$ graphs are comparable except when $\ln s\gg 1$, so that σ_1 is not guaranteed to be positive. If it were found to be negative, then additional Regge-cut graphs would of course have to be included. In practice the cut contribution turns out to be small enough that these additional graphs are not needed.[13]

The contributions of the Regge-cut graphs to the polarization parameters are obtained by substituting Eq. (3.1) into Eqs. (2.5)–(2.7) and using Eq. (3.4). Then the outgoing polarization P_c is

$$P_c\sigma_1=\frac{1}{16\pi s}\frac{1}{(2s_a+1)(2s_b+1)}\int\frac{d^2k_\perp}{16\pi^2}\left\{\sum_{\lambda_a}\mathrm{Re}[(\beta^1_{+\lambda_a}N_{\alpha_2-,\alpha_4\lambda_a}-\beta^1_{-\lambda_a}N_{\alpha_2+,\alpha_4\lambda_a})\xi_1^*\xi_2\xi_4]\right\}$$
$$\times\left(\sum_{\lambda_b}N_{\alpha_3\lambda_b,\alpha_4\lambda_b}\right)g_{12,3}\left(\frac{s}{M^2}\right)^{\alpha_1+\alpha_2+\alpha_4-1}(M^2)^{\alpha_3+\alpha_4-1}. \tag{3.7}$$

The beam-asymmetry parameter Σ_a is

$$\Sigma_a\sigma_1=-\frac{1}{16\pi s}\frac{1}{2s_b+1}\int\frac{d^2k_\perp}{16\pi^2}\left\{\sum_{\lambda_c}\mathrm{Re}[(\beta^1_{\lambda_c+}N_{\alpha_2\lambda_c,\alpha_4-}-\beta^1_{\lambda_c-}N_{\alpha_2\lambda_c,\alpha_4+})\xi_1^*\xi_2\xi_4]\right\}$$
$$\times\left(\sum_{\lambda_b}N_{\alpha_3\lambda_b,\alpha_4\lambda_b}\right)g_{12,3}\left(\frac{s}{M^2}\right)^{\alpha_1+\alpha_2+\alpha_4-1}(M^2)^{\alpha_3+\alpha_4-1}. \tag{3.8}$$

The target-asymmetry parameter Σ_b, which vanished identically for pole graphs, is

$$\Sigma_b\sigma_1=-\frac{1}{16\pi s}\frac{2}{2s_a+1}\int\frac{d^2k_\perp}{16\pi^2}\left[\sum_{\lambda_a\lambda_c}\beta^1_{\lambda_c\lambda_a}\mathrm{Re}(N_{\alpha_2\lambda_c,\alpha_4\lambda_a}\xi_1^*\xi_2\xi_4)\right]\mathrm{Re}(N_{\alpha_3+,\alpha_4-})g_{12,3}\left(\frac{s}{M^2}\right)^{\alpha_1+\alpha_2+\alpha_4-1}(M^2)^{\alpha_3+\alpha_4-1}, \tag{3.9}$$

where the fact that

$$N_{\alpha_3-,\alpha_4+}=N^*_{\alpha_3+,\alpha_4-} \tag{3.10}$$

has been used. Factors of the form $\mathrm{Re}(N_{\alpha_2\lambda_c,\alpha_4\lambda_a}\xi_1^*\xi_2\xi_4)$ appear in each of these formulas. As in the case of σ_1, only the real part of N contributes to the integral, so that the replacement

$$\mathrm{Re}(N_{\alpha_2\lambda_c,\alpha_4\lambda_a}\xi_1^*\xi_2\xi_4)\to\mathrm{Re}(N_{\alpha_2\lambda_c,\alpha_4\lambda_a})\mathrm{Re}(\xi_1^*\xi_2\xi_4) \tag{3.11}$$

can be made in each case.

By parity invariance the Reggeon-particle vertices satisfy

$$N_{\alpha_i\lambda,\alpha_j\mu}=\eta_i\eta_j(-1)^{\lambda-\mu}N_{\alpha_i-\lambda,\alpha_j-\mu}, \tag{3.12}$$

where η_i and η_j are the naturalities of α_i and α_j. Since α_3 and α_4 have natural parity, α_1 and α_2 must then have the same naturality, so that just as for the pole graphs each observable can be written as the sum of a natural-parity and an unnatural-parity part. In particular, if all trajectories have natural parity, then

$$\Sigma_a=P_c. \tag{3.13}$$

If in addition all particles have spin $\frac{1}{2}$, then the formulas for the Regge-cut contributions become

$$\sigma_1=-\frac{2}{16\pi s}\int\frac{d^2k_\perp}{16\pi^2}\mathrm{Im}[(\beta^1_{++}N_{\alpha_2+,\alpha_4+}+\beta^1_{-+}N_{\alpha_2-,\alpha_4+})\xi_1^*\xi_2\xi_4]N_{\alpha_3+,\alpha_4+}g_{12,3}\left(\frac{s}{M^2}\right)^{\alpha_1+\alpha_2+\alpha_4-1}(M^2)^{\alpha_3+\alpha_4-1}, \tag{3.14}$$

$$P_c\sigma_1=\frac{2}{16\pi s}\int\frac{d^2k_\perp}{16\pi^2}\mathrm{Re}[(\beta^1_{++}N_{\alpha_2-,\alpha_4+}-\beta^1_{-+}N_{\alpha_2+,\alpha_4+})\xi_1^*\xi_2\xi_4]N_{\alpha_3+,\alpha_4+}g_{12,3}\left(\frac{s}{M^2}\right)^{\alpha_1+\alpha_2+\alpha_4-1}(M^2)^{\alpha_3+\alpha_4-1}, \tag{3.15}$$

$$\Sigma_b \sigma_1 = -\frac{2}{16\pi s}\int \frac{d^2k_\perp}{16\pi^2}\,\mathrm{Re}[(\beta^1_{++}N_{\alpha_2+,\alpha_4+}+\beta^1_{-+}N_{\alpha_2-,\alpha_4+})\xi_1^*\xi_2\xi_4]$$
$$\times\mathrm{Re}(N_{\alpha_3+,\alpha_4-})\,g_{12,3}\left(\frac{s}{M^2}\right)^{\alpha_1+\alpha_2+\alpha_4-1}(M^2)^{\alpha_3+\alpha_4-1}. \tag{3.16}$$

Formulas for any other special case can also be readily obtained.

B. Absorption model

The Reggeon-particle vertex $N_{\alpha_2\lambda_c,\alpha_4\lambda_a}$ is originally defined as an integral over the full Reggeon-particle amplitude with the contour shown in Fig. 5(a).[19,20] This contour can be distorted as shown in Fig. 5(b) to give

$$N_{\alpha_2\lambda_c,\alpha_4\lambda_a} = \frac{1}{\pi}\int_0^\infty ds'\,\mathrm{Im}A_{\alpha_2\lambda_c,\alpha_4\lambda_a}(s'). \tag{3.17}$$

where $\mathrm{Im}A_{\alpha_2\lambda_c,\alpha_4\lambda_a}(s')$ is the imaginary part of the Reggeon-particle amplitude. In the absorption-model ansatz for $N_{\alpha_2\lambda_c,\alpha_4\lambda_a}$, the sum rule is saturated by the one-particle intermediate state. Thus, for spinless particles

$$N_{\alpha_2,\alpha_4} = \beta_{\alpha_2}(t_2)\beta_{\alpha_4}(t'). \tag{3.18}$$

This ansatz reproduces in the framework of the Reggeon calculus the usual absorption model for two-body amplitudes.[12] (Of course more complicated absorption prescriptions are often used in detailed fits to two-body data, but these prescriptions are generally similar.)

For particles with spin the absorption model is more complicated than Eq. (3.18). The vertex is still obtained by saturating the sum rule with the one-particle intermediate state, giving

$$N_{\alpha_2\lambda_c,\alpha_4\lambda_a} = \sum_{\lambda'}\langle p_c\lambda_c|\,\beta^{(2)}|\,p'\lambda'\rangle\langle p'\lambda'|\,\beta^{(4)}|\,p_a\lambda_a\rangle, \tag{3.19}$$

where p' and λ' are the momentum and helicity of the intermediate particle. However, according to Jacob and Wick,[21] the matrix elements in this equation have phase factors associated with azimuthal rotations. Take $\vec{p}_a$ to be along the z axis, $\vec{p}_c$ to be in the xz plane with polar angle θ, and $\vec{p}'$ to have polar and azimuthal angles θ' and φ', respectively. See Fig. 6. Then the variables used previously are[22]

$$\begin{aligned} t &= -2k_s^2(1-\cos\theta),\\ t' &= -2k_s^2(1-\cos\theta'),\\ t_2 &= -2k_s^2(1-\cos\theta\cos\theta'-\sin\theta\sin\theta'\cos\varphi'),\\ d^2k_\perp &= \tfrac{1}{2}\,dt'\,d\varphi'. \end{aligned} \tag{3.20}$$

The calculation of the phase factors in Eq. (3.19) is straightforward and is carried out in Appendix C. The result is

$$N_{\alpha_2\lambda_c,\alpha_4\lambda_a} = \sum_{\lambda'}(-1)^{\lambda_c-\lambda'}e^{-i(\lambda_c-\lambda')\varphi''}$$
$$\times\beta^{(2)}_{\lambda_c\lambda'}(t_2)e^{-i(\lambda'-\lambda_a)\varphi'}\beta^{(4)}_{\lambda'\lambda_a}(t'), \tag{3.21}$$

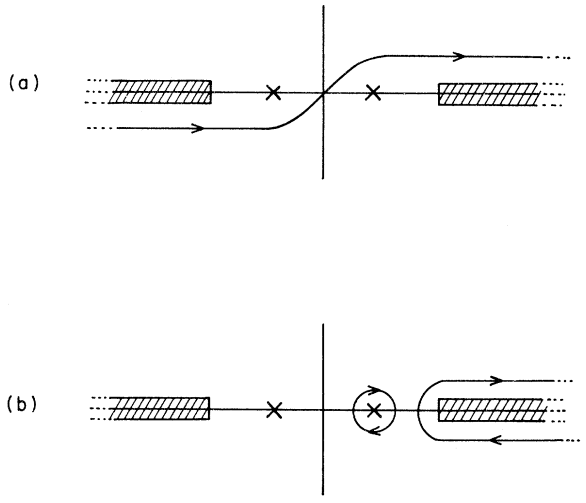

FIG. 5. Contours for Eq. (3.17).

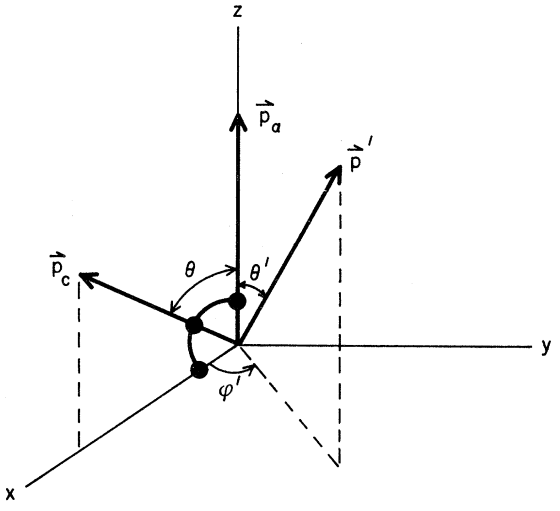

FIG. 6. Definition of the angles θ, θ', and φ'.

where

$$\varphi'' = \tan^{-1}\left(\frac{\cos\frac{1}{2}\theta \sin\frac{1}{2}\theta' \sin\varphi'}{-\sin\frac{1}{2}\theta \cos\frac{1}{2}\theta' + \cos\frac{1}{2}\theta \sin\frac{1}{2}\theta' \cos\varphi'}\right) \tag{3.22}$$

is the azimuthal angle for $\beta^{(2)}$.

If the overall scattering angle is zero, as for $N_{\alpha_3\lambda_b,\alpha_4\lambda_b}$, then the two azimuthal angles are equal. Thus,[18]

$$N_{\alpha_3\lambda_b,\alpha_4\lambda_b} = e^{-i(\lambda_b'-\lambda_b)\varphi'} \sum_{\lambda'} (-1)^{\lambda_b'-\lambda'} \beta^{(3)}_{\lambda_b'\lambda'}(t') \beta^{(4)}_{\lambda'\lambda_b}(t'). \tag{3.23}$$

It should be noted that $\sin\varphi'$ and $\sin\varphi''$ are odd functions of φ' while $\cos\varphi'$, $\cos\varphi''$, and all momentum transfers are even functions. Thus justifies the assertion made in Eq. (3.6) and Eq. (3.11) that the imaginary part of $N_{\alpha_2\lambda_c,\alpha_4\lambda_a}$ does not contribute to the cross section or the single polarizations.

If the absorption model for the Reggeon-particle vertices is used, then the Regge-cut amplitude is expressed in terms of two-body Regge residues and the nonforward triple-Regge vertex $g_{12,3}(t_1, t_2, t_3)$. At $t_3 = 0$ this vertex is just that measurable in inclusive reactions. For fixed t_1 and t_2 its dependence on t_3 is presumably similar to that of an ordinary two-body residue. Thus while $g_{12,3}(t_1, t_2, t_3)$ is not precisely known, it is strongly constrained, so a reasonable estimate of the Regge graph can be made.

IV. SPECIFIC REACTIONS AND NUMERICAL RESULTS

The purpose of this section is to give final expressions for P_c, Σ_a, and Σ_b after the Gribov N functions have been replaced by their appropriate absorption-model prescriptions, and also to present numerical results which can be compared to the available experimental data. In so doing, we make assumptions about the values of certain parameters which we believe are reasonable and conform with what we know from two-body phenomenology. General expectations of the behavior of the single-spin observables are given in Tables I and II.

A. Unpolarized cross section σ

In an earlier paper,[13] we estimated the cut contributions to the unpolarized inclusive cross sections in the triple-Regge region for $\pi^- p \to \pi^0 X$, $\pi^- p \to \eta X$, and $K^- p \to \bar{K}^0 X$ and found these contributions to be about 30% of the pole contributions for $-t \leq 0.4$ (GeV/c)^2. The charge- and hypercharge-exchange inclusive processes under consideration here have comparable cut contributions to their unpolarized inclusive cross sections. Since our estimates of the single-spin observables can be reliable only for small values of momentum transfer t, it is a reasonable approximation to drop the small cut contribution to the unpolarized inclusive cross section σ_1. In the expressions given below for P_c, Σ_a, and Σ_b, we have therefore replaced σ_1 by σ_{pole}. Since the present triple-Regge analyses[1] cannot isolate the individual triple-Regge couplings such as $G_{\rho\rho P}$, $G_{A_2A_2P}$, $G_{K^*K^*P}$, $G_{K^{**}K^{**}P}$, etc., we assume that

$$G_{\rho\rho P} = G_{A_2A_2P} = G_{RRP} \tag{4.1}$$

and

$$G_{K^*K^*P} = G_{K^{**}K^{**}P} = G'_{RRP}. \tag{4.2}$$

Again, this is a reasonable assumption to make in the face of lack of any other alternative which is better and at the same time uncontroversial. Note that we do not assume that G_{RRP} and G'_{RRP} are equal or that either of them is the G_{MMP} used in triple-Regge pole phenomenology. Since in all the reactions under consideration the dominant Regge poles are either $(\rho\rho P)$ and (A_2A_2P) or (K^*K^*P) and $(K^{**}K^{**}P)$, we have

$$\sigma_{\text{pole}} = \frac{2}{s} G_{RRP}(t, t, 0)\left(\frac{s}{M^2}\right)^{2\alpha(t)} (M^2)^{\alpha_P(0)}, \tag{4.3}$$

where we assumed that $\tau = \pm$ Regge poles are approximately exchange degenerate.

B. Polarization of the outgoing particle P_C

At the present time, inclusive polarization data are available on some of the charge- and hypercharge-exchange reactions given in Table III. For relatively high energies, the important triple-Regge pole graphs are the scaling contributions such as (ρ, ρ, P) and (A_2, A_2, P) or (K^*, K^*, P) and (K^{**}, K^{**}, P). In the same energy region, the important cut graphs are (ρ, ρ, P, P) and (A_2, A_2, P, P) or (K^*, K^*, P, P) and (K^{**}, K^{**}, P, P) in the notation explained in Sec. III. We restrict our attention here to such scaling graphs, although we recognize that for most of the existing data the energy is relatively low, so that some of the nonscaling terms listed in Tables I and II may be important.

The contribution of the (R, R, P, P) graph to P_c is given by Eq. (3.15) with $\alpha_1 = \alpha_2 = \alpha$ and $\alpha_3 = \alpha_4 = \alpha_P$. For the Gribov N functions we use the ab-

TABLE II. Dominant graphs for Σ_b. We list what we expect to be the dominant graphs for σ_1 and for Σ_b in the triple-Regge region. Pole graphs are labeled by $\alpha_1\alpha_2\alpha_3$, cut graphs by $\alpha_1\alpha_2\alpha_3\alpha_4$. M refers to any of the ω, f, ρ, A_2 Regge poles. The behavior given is that of the invariant cross section σ_1 or $\Sigma_b\sigma_1$ assuming that $\alpha_P=1$, $\alpha_M=\frac{1}{2}$, $\alpha_{K^*}=\frac{1}{4}$ and ignoring logarithms.

Reaction	Graph	Behavior	Comments
$\pi^- p \to \pi^0 X$	$\rho\rho P$	$(1-x)^0(s)^0$	$\Sigma_b=0$; dominates σ_1
	$\rho\rho P\rho$	$(1-x)^0(s)^{-1/2}$	$\Sigma_b\neq 0$
	$\rho\rho\rho P$	$(1-x)^{-1/2}(s)^{-1/2}$	$\Sigma_b\neq 0$; $\rho\rho\rho$ vertex needed
$\pi^- p \to \eta X$	A_2A_2P	$(1-x)^0(s)^0$	$\Sigma_b=0$; dominates σ_1
	$A_2A_2P\rho$	$(1-x)^0(s)^{-1/2}$	$\Sigma_b\neq 0$
	$A_2A_2\rho P$	$(1-x)^{-1/2}(s)^{-1/2}$	$\Sigma_b\neq 0$; $A_2A_2\rho$ vertex needed
$pp\to pX$, $\pi^\pm p\to \pi^\pm X$, $K^\pm p\to K^\pm X$	PPP	$(1-x)^{-1}(s)^0$	$\Sigma_b=0$; dominates σ_1 for $x\gtrsim 0.9$
	MMP	$(1-x)^0(s)^0$	$\Sigma_b=0$; dominates σ_1 for $x\lesssim 0.9$
	$PPP\rho, PPPA_2$	$(1-x)^{-1}(s)^{-1/2}$	$\Sigma_b\neq 0$
	$MMP\rho, MMPA_2$	$(1-x)^0(s)^{-1/2}$	$\Sigma_b\neq 0$
	$P\rho\rho P, PA_2A_2P$	$(1-x)^{-1}(s)^{-1/2}$	$\Sigma_b\neq 0$; nondiagonal triple-Regge vertex
	$f\rho\rho P$, etc.	$(1-x)^{-1/2}(s)^{-1/2}$	$\Sigma_b\neq 0$; nondiagonal triple-Regge vertex
$pp\to(\Lambda,\Sigma^0)X$	$K^*K^*P, K^{**}K^{**}P$	$(1-x)^{1/2}(s)^0$	$\Sigma_b=0$; dominates σ_1
	$K^*K^*P\rho, K^{**}K^{**}P\rho$, $K^*K^*PA_2, K^{**}K^{**}PA_2$	$(1-x)^{1/2}(s)^{-1/2}$	$\Sigma_b\neq 0$
	$K^*K^*\rho P, K^{**}K^{**}\rho P$, $K^*K^*A_2P, K^{**}K^{**}A_2P$	$(1-x)^0(s)^{-1/2}$	$\Sigma_b\neq 0$; $K^*K^*\rho$, etc., vertices needed

sorption-model prescription, Eq. (3.23), together with the standard assumption that the Pomeron conserves s-channel helicity. For the unpolarized cross section we take just the pole graphs. Then, adding the cut graphs with positive- and negative-signature meson trajectories and using Eqs. (4.1) and (4.2), we find that

$$P_c = -\frac{1}{32\pi^2}\int_{-\infty}^{0} dt' \int_0^{2\pi} d\varphi' \left(\frac{\mathrm{Re}[\xi_+^*(t)\xi_+(t_2)\xi_P(t')]}{\mathrm{Re}[\xi_+^*(t_2)\xi_+(t)]} + \frac{\mathrm{Re}[\xi_-^*(t)\xi_-(t_2)\xi_P(t')]}{\mathrm{Re}[\xi_-^*(t_2)\xi_-(t)]} \right)$$

$$\times \frac{G_{RRP}(t,t_2,t')}{G_{RRP}(t,t,0)}\,\beta_{++}^{aP}(t')\,\frac{[\beta_{++}^R(t)\beta_{-+}^R(t_2)\cos\varphi'' + \beta_{++}^R(t_2)\beta_{-+}^R(t)]}{[\beta_{++}^R(t_2)\beta_{++}^R(t) + \beta_{-+}^R(t_2)\beta_{-+}^R(t)]}\,\beta_{++}^{bP}(t')$$

$$\times \left(\frac{s}{M^2}\right)^{\alpha(t_2)-\alpha(t)+\alpha_P(t')-1} (M^2)^{2\alpha_P(t')-2}, \tag{4.4}$$

TABLE III. Reggeon-particle couplings for specific reactions. The Pomeron residues are obtained from the total cross sections with positive beams.

Reaction	γ_a^P	γ_b^P	ρ_R
$\pi^\pm p \to \Lambda^0 X$	10.14	5.88	−2.11
$\pi^\pm p \to \Sigma^0 X$	10.14	5.88	1.96
$K^\pm p \to \Lambda^0 X$	10.14	4.41	−2.11
$K^\pm p \to \Sigma^0 X$	10.14	4.41	1.96
$pp \to \Lambda^0 X$	10.14	10.14	−2.11
$pp \to \Sigma^0 X$	10.14	10.14	1.96
$\Sigma^- p \to \Lambda^0 X$	8.62	10.14	12.31
$\Sigma^- p \to \Sigma^0 X$	8.62	10.14	−0.82

where we have assumed exchange degeneracy. Note that in this expression for P_c, $G_{RRP}(t, t_2, t')$ is a triple-Regge coupling which is not directly amenable to experimental determination. However, for $t_2 \to t$ and $t' \to 0$, $G_{RRP}(t, t_2, t') \to G_{RRP}(t, t, 0)$, which is the triple-Regge coupling which appears in the expression for the triple-Regge pole graph. It is clear that we must make some assumption about the extension of the familiar $G_{RRP}(t, t, 0)$ to nonzero momentum transfer in the third Reggeon leg. If we parametrize $G_{RRP}(t, t, 0)$ as

$$G_{RRP}(t, t, 0) = G_0 e^{at}, \tag{4.5}$$

a reasonable guess for $G_{RRP}(t, t_2, t')$ is

$$G_{RRP}(t, t_2, t') = G_0 e^{a(t+t_2)/2 + b_R t'}. \tag{4.6}$$

In our calculation, we use this parametrization and take a from the triple-Regge analysis. While we do not know b_R, we assume that it is comparable to the slope of a typical Pomeron residue. Furthermore, note that G_0 cancels out in one expression for P_c. Now if we parameterize the Regge residues as

$$\begin{aligned} \beta^{aP}_{++}(t') &= \gamma_a^P e^{b_a t'}, \\ \beta^{bP}_{++}(t') &= \gamma_b^P e^{b_b t'}, \\ \beta^{R}_{++}(t) &= \gamma^R_{++} e^{R_{++} t}, \\ \beta^{R}_{-+}(t) &= \sqrt{-t}\, \gamma^R_{-+} e^{R_{-+} t}, \end{aligned} \tag{4.7}$$

and assume that $R_{++} \approx R_{-+} \approx b_R$, the final expression for P_c is

$$\begin{aligned} P_c = -\frac{1}{32\pi^2} \rho_R \gamma_a^P \gamma_b^P \int_0^{t_0} dt' \int_0^{2\pi} d\varphi'\, & e^{(b_a + b_b + b_R + a/2)t' - a(tt')^{1/2}\cos\varphi'} \\ & \times \frac{[(-t_2)^{1/2}\cos\varphi'' + (-t)^{1/2}]}{[1 + (tt_2)^{1/2}\rho_R{}^2]} s^{2\alpha_P t'} \left(\frac{1}{1-x}\right)^{-\alpha'_P t' + \alpha'_M (t' - 2(tt')^{1/2}\cos\varphi')} \\ & \times \left\{ \frac{\mathrm{Re}[\xi^*_+(t)\xi_+(t_2)\xi_P(t')]}{\mathrm{Re}[\xi^*_+(t_2)\xi_+(t)]} + \frac{\mathrm{Re}[\xi^*_-(t)\xi_-(t_2)\xi_P(t')]}{\mathrm{Re}[\xi^*_-(t_2)\xi_-(t)]} \right\}, \end{aligned} \tag{4.8}$$

where

$$\rho_R = \gamma^R_{-+}/\gamma^R_{++},$$

and φ'' is given by Eq. (3.22).

C. Polarized-beam asymmetry Σ_a

For natural-parity Regge poles and for the cut graphs we have considered in the calculation of P_c,

$$\Sigma_a \equiv P_c. \tag{4.9}$$

D. Polarized-target asymmetry Σ_b

As pointed out earlier, the polarized-target asymmetry vanishes identically for triple-Regge pole graphs in a factorizable Regge-pole model.[9] Therefore, a nonzero polarized-target asymmetry can only arise from Regge-cut graphs such as we have considered before in connection with P_c and Σ_a. From Eq. (3.16) we note that the cut graphs contributing to Σ_b must have helicity flip at the $b \to b'$ vertex. Hence the dominant graphs contributing to Σ_b must have at least one of α_3 or α_4 trajectories from ρ, A_2, K^*, K^{**}, etc. which have dominant flip coupling.[12] This empirical fact restrict somewhat the number of graphs one has to consider to estimate the size of Σ_b for a given process. A general discussion of polarized-target asymmetries from various processes is given in Table II. Experimentally, nothing is known about the size of Σ_b for any processes from Table II except for $\pi^\pm p \to \pi^\pm X$. These measurements[23] show fairly large target asymmetry for $x \geq 0.75$. However, this region corresponds to $M^2 \lesssim 4$ (GeV)^2, so nonscaling terms and/or resonance contributions are likely to be the main contributor to the asymmetry. We can hardly hope that our triple-Regge-region formalism will make any sense down to M^2 values as low as 4 (GeV)^2 except, perhaps, in some average sense. The leading cut graphs for $\Sigma_b(\pi^\pm p \to \pi^\pm X)$ are expected to be (P, P, P, ρ^0) and $(\rho^0, \rho^0, P, \rho)$. Note that there is no $(\rho^0, \rho^0, \rho^0, P)$ graph by isospin. Graphs such

as (ρ^0, P, ρ^0, P) with nondiagonal triple-Regge vertices, and, at low energies, graphs such as (P, P, f, ρ^0) might also be important. Note that all these graphs, except the nondiagonal one, have an odd number of ρ^0 connected to the pions. Since $C_{\rho 0} = -1$, these graphs will give mirror symmetry between π^+ and π^- on a polarized nucleon target.

Since the polarized-target asymmetries may provide us with a useful tool for teaching us something about the size and importance of Regge-cut corrections in inclusive reactions, we should look for a process which can be measured experimentally and to which relatively few cut graphs contribute so that it can be calculated theoretically with fewer assumptions. $\pi^- p \to \pi^0 X$ is one such process. Important cut graphs are $(\rho^-\rho^-, P, \rho^0)$ and $(\rho^-\rho^-, \rho^0, P)$, and their contributions to the polarized-target asymmetry, called Σ^{I} and Σ^{II}, respectively are

$$\Sigma_b^{\mathrm{I}} = -\frac{1}{s}\int \frac{dt'\,d\varphi'}{32\pi^2}\cos\varphi' \frac{\mathrm{Re}[\xi_\rho^*(t)\xi_\rho(t_2)\xi_\rho(t')]}{\mathrm{Re}[\xi_\rho^*(t)\xi_\rho(t)]}\beta^{\rho^0}_{\pi^-\pi^-}(t')\frac{G_{\rho\rho P}(t,t_2,t')}{G_{\rho\rho P}(t,t,0)}\beta^{\rho^0}_{+-}(t') \times\left(\frac{s}{M^2}\right)^{\alpha_\rho(t_2)+\alpha_\rho(t')-\alpha_\rho(t)}(M^2)^{\alpha_\rho(t')+\alpha_P(t')-1}, \tag{4.10}$$

$$\Sigma_b^{\mathrm{II}} = \frac{1}{s}\int \frac{dt'\,d\varphi'}{32\pi^2}\frac{\mathrm{Re}[\xi_\rho^*(t)\xi_\rho(t_2)\xi_P(t')]}{\mathrm{Re}[\xi_\rho^*(t)\xi_\rho(t_2)]}\beta^{P}_{\pi^-\pi^-}(t')\frac{G_{\rho\rho\rho}(t,t_2,t')}{G_{\rho\rho P}(t,t,0)} \times\frac{\beta^{\rho^0}_{+-}(t')}{\beta^{\rho^0}_{++}(t')}\beta^{bP}_{++}(t')\left(\frac{s}{M^2}\right)^{\alpha_\rho(t_2)+\alpha_P(t')-\alpha_\rho(t)}(M^2)^{\alpha_\rho(t')+\alpha_\rho(t')-1}, \tag{4.11}$$

where

$$G_{\rho\rho P}(t,t_2,t') = \frac{1}{16\pi}\mathrm{Re}[\xi_\rho^*(t)\xi_\rho(t_2)]\beta^{\rho}_{\pi^0\pi^-}(t)\beta^{\rho}_{\pi^0\pi^-}(t_2)g_{\rho\rho P}(t,t_2,t')\beta^{bP}_{++}(t'), \tag{4.12}$$

where

$$G_{\rho\rho\rho}(t,t_2,t') = \frac{1}{16\pi}\mathrm{Re}[\xi_\rho^*(t)\xi_\rho(t_2)]\beta^{\rho}_{\pi^0\pi^-}(t)\beta^{\rho}_{\pi^0\pi^-}(t_2)g_{\rho\rho\rho}(t,t_2,t')\beta^{b\rho}_{++}(t'). \tag{4.13}$$

In arriving at these expressions, we have used the absorption-model prescription given in Eqs. (3.21) and (3.23) and the definition of Σ_b given in Eq. (3.16). We have also divided the expression on both sides of Eq. (3.16) by

$$\sigma \cong \sigma_{\mathrm{pole}} = \frac{1}{s}G_{\rho\rho P}(t,t,0)\left(\frac{s}{M^2}\right)^{2\alpha_\rho(t)}(M^2)^{\alpha_P(0)}. \tag{4.14}$$

The rationale for doing this was explained earlier. Since the triple-Regge couplings which appear in the expression for Σ_b^{I} and Σ_b^{II} are not known very well, we will not attempt to give any numerical estimate of the polarized-target asymmetry. The reader may wish to make such an estimate for himself.

E. Numerical results

We estimate $P_c(s,x,t)$ using Eq. (4.8) and evaluating the integral numerically. For the exchange-degenerate meson trajectory we take

$$\alpha_+(t) = \alpha_-(t) = \alpha(t) = 0.5 + 0.9t, \tag{4.15}$$

and for the Pomeron trajectory,[24]

$$\alpha_P(t) = 1.0 + 0.28t. \tag{4.16}$$

The parameter a is obtained by taking the logarithmic derivative of the MMP coupling[25] in $pp \to pX$. The parameters b_a, b_b, and b_R always appear in the combination $b_a + b_b + b_R$, and for this we take

$$b_a + b_b + b_R = 6\ \mathrm{GeV}^{-2}.$$

A slight variation of the number on the right-hand side changes the result by an insignificant amount.

The values of ρ_R for vector trajectories are obtained from the known values for the ρNN couplings,[25] and the same values are assumed for the tensor trajectories. These and other parameters are listed in Table III.

Our predictions based on the cut graphs for

$$P(s,x) = \frac{\int_{-\infty}^{0} dt\, P_c(s,x,t)\sigma_1(s,x,t)}{\int_{-\infty}^{0} dt\,\sigma_1(s,x,t)} \tag{4.17}$$

are compared with the experimental data in Figs. 7 and 8 for $p\pi^+ \to \Lambda X$ at 18.5 GeV/c,[26] $p\pi^- \to \Lambda X$ at 18.5 GeV/c,[26] and $pK^- \to \Lambda X$ at 14.3 GeV/c.[27] These data are generally in agreement with our predictions of small polarizations, although at

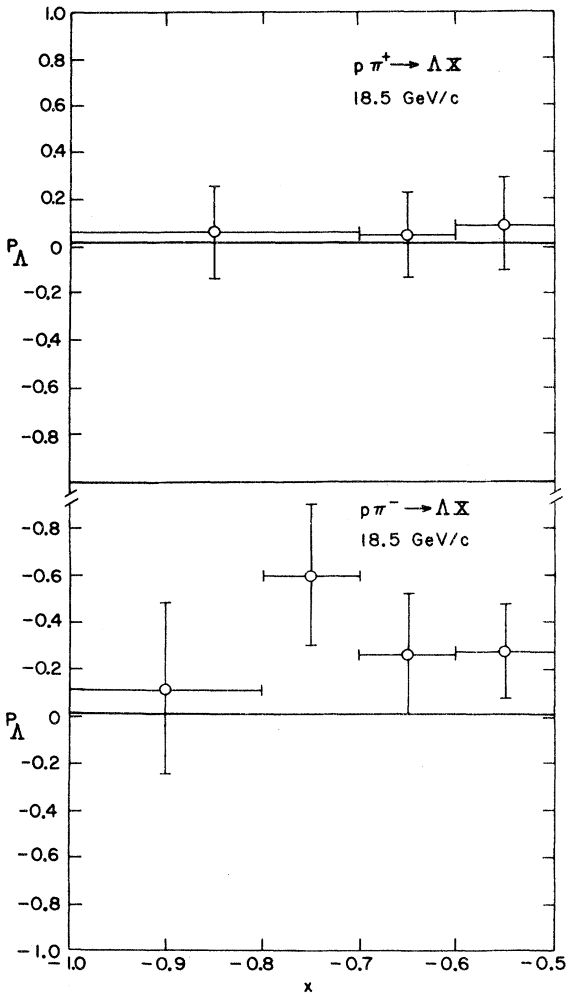

FIG. 7. P_Λ for $p\pi^\pm \to \Lambda X$. Data are from Ref. 26.

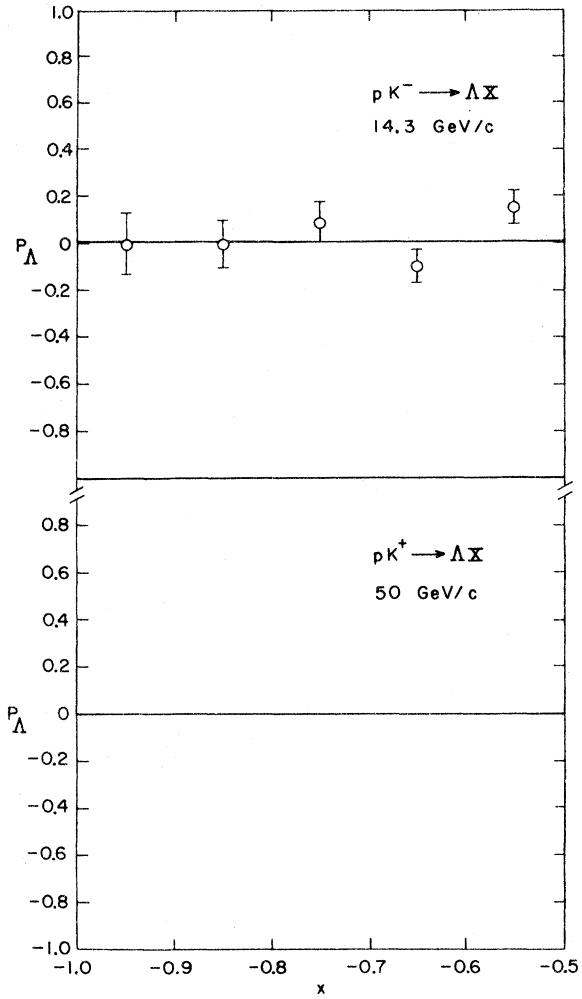

FIG. 8. P_Λ for $pK^\pm \to \Lambda X$. Data are from Ref. 27.

such low energies the neglect of nonscaling graphs is questionable. We also give predictions for $P(s,x)$ for $pK^+ \to \Lambda X$ at 50 GeV/c, $pp \to \Lambda X$ at 50 GeV/c, and $\Sigma^- p \to \Lambda^0 X$ at 23 GeV/c in Figs. 8 and 9. (The last of these will be measured in an ongoing hyperon-beam experiment at BNL.[28]) A measurement of $P_\Lambda(s,x)$ in $pp \to \Lambda X$ at 205 GeV has also been published.[29] The statistics are very poor, but the data are consistent with zero, and our calculation also gives negligible polarization.

V. CONCLUSION

We have calculated what we believe to be the most important Regge-cut contributions to the polarization parameters P_c, Σ_a, and Σ_b for large x and high energy. We find that while these graphs do give contributions which scale within logarithms, the magnitudes of the polarizations are quite small, in general less than 5%. Thus, even if the contributions of other graphs are included, it seems unlikely that there could be any substantial polarization at high energy. In contrast to two-body reactions, the smallness of the polarization is not simply a consequence of helicity conservation for the Pomeron. Rather, it arises from the intrinsic smallness of Pomeron cuts and from the fact that absorption changes the phase of a Regge pole only slightly.

At lower energies a variety of triple-Regge pole graphs can contribute to P_c and Σ_a. With the possible exception of the $K^*K^{**}P$ graph, all should give polarizations which behave like $(s)^{-1/2}$ at fixed x. While we have not calculated the cut graphs which behave like $(s)^{-1/2}$, we do not expect that they are very important. Thus, it is appropriate to analyze polarization data at moderate

energies in terms of just the pole graphs. Such data and analysis would be interesting because it would provide information about nondiagonal triple-Regge vertices and further test the whole triple-Regge framework.

Note added in proof. The polarization in $pp \to \Lambda X$ at $p_{\text{lab}} = 300$ GeV/c has been measured recently.[30] The polarization for $x = 0.7$, the largest available value, is found to increase with $|t|$; it is about 7% at $t = -0.5$ GeV^2. This is larger than the contribution from the cut graphs which we have considered. However, other graphs, particularly the $K^*K^{**}P$ pole graph, might also be present; see Table I.

ACKNOWLEDGMENT

We wish to thank Dr. T. L. Trueman and Dr. G. C. Fox for useful discussions and encouragement throughout the course of this work.

APPENDIX A: SPIN STRUCTURE OF INCLUSIVE REACTIONS

Consider the one-particle inclusive reaction

$$a + b \to c + X, \tag{A1}$$

where X stands for everything in the final state besides the observed particle c. Let a, b, and c have spins s_a, s_b, s_c and helicities λ_a, λ_b, and λ_c in the s-channel center-of-mass frame. Let λ_X denote the helicity of the multiparticle state X. Our normalization convention is such that the spin-averaged invariant cross section is given by

$$s\frac{d^2\sigma}{dt\,dM^2} = \frac{1}{(2s_a+1)(2s_b+1)} \sum_{\lambda_a,\lambda_b,\lambda_c} \sum_{i=1}^{\infty} \sum_{\lambda_{X_i}} \int d\Phi_i \left| f_{\lambda_c\lambda_{X_i},\lambda_a\lambda_b}(s,t,M_{X_i}{}^2)\right|^2, \tag{A2}$$

where

$$f_{\lambda_c\lambda_{X_i},\lambda_a\lambda_b}(s,t,M_{X_i}{}^2)$$

is the amplitude[21] for the process shown in Eq. (A1) and the integration is over the phase space of the multiparticle state $\{X_i\}$. As shown by Mueller,[8] the right-hand side of the above equation can be related to the discontinutiy in the missing mass $M_X{}^2$ of the forward $3 \to 3$ scattering amplitude using a generalized optical theorem as follows:

$$\frac{1}{2i}\,\mathrm{Disc}_{M_X{}^2} F_{\lambda_a'\lambda_b'\lambda_c'\lambda_a\lambda_b\lambda_c}(s,t,M_X{}^2) = \sum_i \sum_{\lambda_{X_i}} \int d\Phi_i f_{\lambda_c\lambda_{X_i},\lambda_a\lambda_b}(s,t,M_X{}^2) f^*_{\lambda_c'\lambda_{X_i},\lambda_a\lambda_b}(s,t,M_x{}^2)$$

$$= A_{\lambda_a'\lambda_b'\lambda_c',\lambda_a\lambda_b\lambda_c}(s,t,M_X{}^2). \tag{A3}$$

In terms of this absorptive part $A_{\lambda_a'\lambda_b'\lambda_c',\lambda_a\lambda_b\lambda_c}$, the spin-averaged invariant distribution is given by

$$s\frac{d\sigma}{dt\,dM_X{}^2} = \frac{1}{(2s_a+1)(2s_b+1)} \sum_{\lambda_a,\lambda_b,\lambda_c} A_{\lambda_a\lambda_b\lambda_c,\lambda_a\lambda_b\lambda_c}(s,t,M_X{}^2). \tag{A4}$$

Next we turn to the definition of spin observables for an inclusive reaction in terms of the Mueller amplitudes $A_{\lambda_a'\lambda_b'\lambda_c',\lambda_a\lambda_b\lambda_c}$. Let us assume that both the beam (a) and the target (b) particles are polarized so that their initial state is described by the initial-state density matrix

$$\rho^i_{\lambda_a\lambda_a',\lambda_b\lambda_b'}(A,B) = \rho^A_{\lambda_a\lambda_a'}\rho^B_{\lambda_b\lambda_b'}, \tag{A5}$$

where for spin $\frac{1}{2}$

$$\rho = \tfrac{1}{2}(1 + \vec{\sigma}\cdot\vec{\mathrm{P}}). \tag{A6}$$

The density matrix of the outgoing particle (c) is then

$$\rho^f_{\lambda_c\lambda_c'}(A,B) = \sum_i \sum_{\lambda_a,\lambda_b,\lambda_a'\lambda_b'} \sum_{\lambda_{X_i}} \int d\Phi_i [f_{\lambda_c\lambda_{X_i},\lambda_a\lambda_b}\rho^i_{\lambda_a\lambda_a',\lambda_b\lambda_b'}(A,B) f_{\lambda_c'\lambda_{X_i},\lambda_a\lambda_b}]$$

$$\equiv \sum_{\lambda_a,\lambda_b,\lambda_a',\lambda_b'} A_{\lambda_a'\lambda_b'\lambda_c',\lambda_a\lambda_b\lambda_c}\rho^i_{\lambda_a\lambda_a',\lambda_b\lambda_b'}(A,B). \tag{A7}$$

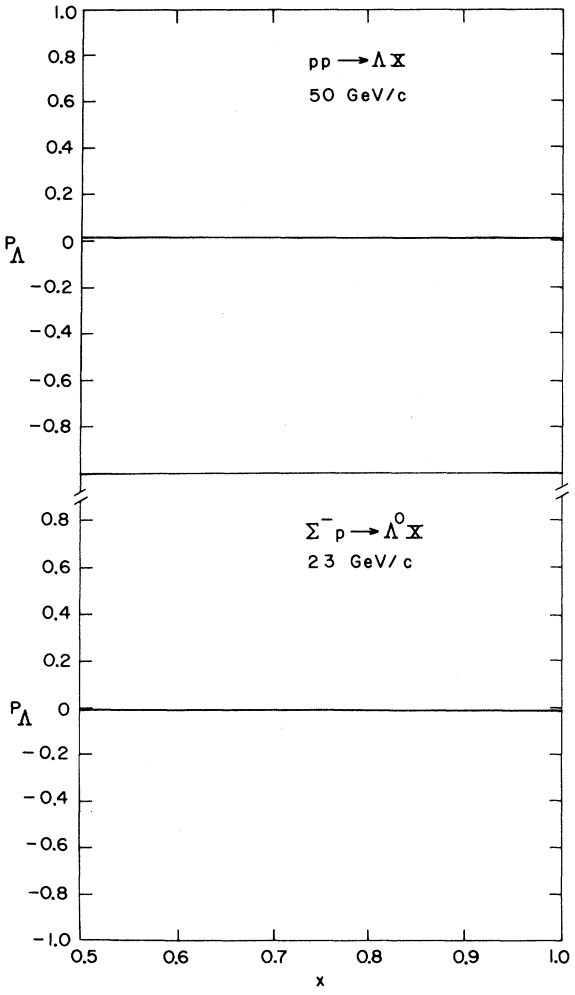

FIG. 9. P_Λ for $pp \to \Lambda X$ and for $\Sigma^- p \to \Lambda X$.

The relation between the density matrix ρ^f and the invariant cross section is

$$s\frac{d\sigma}{dt\,dM^2} = \mathrm{Tr}(\rho^f). \tag{A8}$$

Let us consider several special cases of our general definitions:

(i) unpolarized beam

$$\rho^i_{\lambda_a\lambda_a',\lambda_b\lambda_b'}(0,B) = \frac{1}{(2s_a+1)}\,\delta_{\lambda_a\lambda_a'}\,\frac{1}{(2s_b+1)} \times (1+\vec{\sigma}\cdot\vec{P}_B)_{\lambda_b\lambda_b'}, \tag{A9}$$

(ii) unpolarized target

$$\rho^i_{\lambda_a\lambda_a',\lambda_b\lambda_b'}(A,0) = \frac{1}{(2s_a+1)}\,(1+\vec{\sigma}\cdot\vec{P}_A)_{\lambda_a\lambda_a'} \times \frac{1}{(2s_b+1)}\,\delta_{\lambda_b\lambda_b'}, \tag{A10}$$

(iii) unpolarized beam and target

$$\rho^i_{\lambda_a\lambda_a',\lambda_b\lambda_b'}(0,0) = \frac{1}{(2s_a+1)}\,\delta_{\lambda_a\lambda_a'}\,\frac{1}{(2s_b+1)}\,\delta_{\lambda_b\lambda_b'}. \tag{A11}$$

With these facts in mind, it is straightforward to define any spin observable by taking the appropriate trace of ρ^f with the relevant Pauli matrix. As is well known from two-body physics, parity conservation in the production process imposes relations among various helicity amplitudes and, therefore, leads to vanishing of certain components of polarization vectors. Parity transformation properties of the Mueller amplitudes immediately follow from Eq. (A3) and the transformation law of the exclusive helicity amplitudes. A consequence of the parity invariance is the vanishing of all but the components normal to the scattering plane of the single polarization vectors P_c, Σ_a, and Σ_b, which are the polarization of the outgoing particle c, polarized-beam asymmetry and polarized-target asymmetry, respectively. These observables are defined, in terms of the Mueller amplitudes, as follows:

$$P_c\sigma = (-\tfrac{1}{4}i)\sum_{\lambda_a\lambda_b}(A_{\lambda_a\lambda_b+,\lambda_a\lambda_b-} - A_{\lambda_a\lambda_b-;\lambda_a\lambda_b+}) = \tfrac{1}{2}\sum_{\lambda_a\lambda_b}\mathrm{Im}A_{\lambda_a\lambda_b+,\lambda_a\lambda_b-}, \tag{A12}$$

$$\Sigma_a\sigma = (\tfrac{1}{4}i)\sum_{\lambda_b\lambda_c}(A_{+\lambda_b\lambda_c,-\lambda_b\lambda_c} - A_{-\lambda_b\lambda_c,+\lambda_b\lambda_c}) = \tfrac{1}{2}\sum_{\lambda_b\lambda_c}\mathrm{Im}A_{-\lambda_b\lambda_c,+\lambda_b\lambda_c}, \tag{A13}$$

$$\Sigma_b\sigma = (\tfrac{1}{4}i)\sum_{\lambda_a\lambda_c}(A_{\lambda_a+\lambda_c,\lambda_a-\lambda_c} - A_{\lambda_a-\lambda_c,\lambda_a+\lambda_c}) = \tfrac{1}{2}\sum_{\lambda_a\lambda_c}\mathrm{Im}A_{\lambda_a-\lambda_c,\lambda_a+\lambda_c}. \tag{A14}$$

In these equations, the second relation is a consequence of parity invariance. Furthermore, in the definition of P_c, Σ_a, and Σ_b, we always use the "particle-one" convention of Jacob and Wick for that particle whose spin dependence is being considered. Definition of double- and triple-correlation parameters for inclusive reactions is straightforward, although some care must be exercised for particles having a "particle-two" convention.

APPENDIX B: REGGE CUTS IN THE TRIPLE-REGGE REGION

The purpose of this appendix is to derive an expression for the Regge-cut graph used in this paper for the calculation of various polarization

asymmetries. This is one of the many graphs studied extensively by Abarbanel, Bartels, Bronzan, and Sidhu[17] in their derivation of the Reggeon calculus rule in the triple-Regge region. Throughout this appendix, we will try to follow the relevant section of this reference closely and later on give changes necessary for the labeling of external particle momenta to conform to the notation used in this paper.

Consider the six-point function, T_6, which is an amplitude for the scattering of spinless particles

$$p_1 + p_2 + p_3 \to p_1' + p_2' + p_3' . \tag{B1}$$

In particular, we are only interested in the triple-Regge limit of T_6 which will be defined shortly. Complications arising from the spins of the external particles are discussed in the main text of this paper. We use the following (overcomplete) set of variables for T_6:

$$\begin{aligned} s_{12} &= (p_1 + p_2)^2, \\ s_{13} &= (p_1' + p_3')^2, \\ s_1 &= (p_1 - Q_2)^2, \\ s_{23} &= (p_3 - p_2')^2, \\ s_2 &= (p_2 + Q_1)^2, \\ s_3 &= (p_3 - Q_2)^2, \\ t_i &= Q_i^{\,2} = (p_1 - p_i')^2, \quad i = 1, 2, 3. \end{aligned} \tag{B2}$$

Since T_6 can depend on only eight independent variables, one of these must be eliminated through some constraint. Later on, we will indicate how this six-point function is related to the invariant cross section. The triple-Regge limit of interest is defined as

$$s_{12}, s_{13}, s_1, \frac{s_{12}}{s_1}, \frac{s_{13}}{s_1} \to \infty, \tag{B3}$$

while

$$\frac{s_{13}}{s_{12}} \equiv R, \; s_2, \; s_3, \; s_{23}, \text{ and the } t_i \tag{B4}$$

are all held fixed.

After defining these variables, we express all of the momentum vectors associated with lines inside the hybrid Feynman graph in terms of Sudakov variables, i.e., their components along vector $\tilde{p}_1$ and $\tilde{p}_2$ which carry the "large" components of momenta and along the remaining spacelike two-dimensional vectors perpendicular to $\tilde{p}_i$. The "large" vectors $\tilde{p}_i$ are defined as

$$\tilde{p}_1 = p_1 - \frac{m^2}{s_{12}} p_2, \tag{B5}$$

$$\tilde{p}_2 = p_2 - \frac{m^2}{s_{12}} p_1, \tag{B6}$$

where $p_i^{\,2} = p_i'^{\,2} = m^2$, which are the mass-shell conditions of the external particles. It is clear from the above definitions that $\tilde{p}_1$ lies *mostly* along p_1, the *beam* direction, and that $\tilde{p}_2$ lies mostly along p_2. These redefined momentum vectors, $\tilde{p}_1$, have the property that to order $(1/s_{12})$, $\tilde{p}_i^{\,2} = 0$, so that in the evaluation of our hybrid Feynman graphs to order $1/s$ we may systematically drop $\tilde{p}_i^{\,2}$. We shall see that introducing the Sudakov variables allows one to carry out the integrations over the projection of loop momenta on the $\tilde{p}_i$, leaving one with only the two-dimensional integrals over transverse dimensions. Decompose all vectors in terms of Sudakov variables as

$$V = A\tilde{p}_1 + B\tilde{p}_2 + V_T \tag{B7}$$

with

$$V_\perp \cdot \tilde{p}_1 = V_T \cdot \tilde{p}_2 = 0, \tag{B8}$$

$$V_T^{\,2} \leq 0. \tag{B9}$$

The decomposition of the external vectors is then

$$p_1 = \tilde{p}_1 + \frac{m^2}{s_{12}} \tilde{p}_2, \tag{B10}$$

$$p_2 = \tilde{p}_2 + \frac{m^2}{s_{12}} \tilde{p}_1, \tag{B11}$$

$$p_3 = \left(\frac{m^2 - s_{23} - m^2 R + s_3 - t_2}{s_{12}} \right) \tilde{p}_1 + R\,\tilde{p}_2 + p_{3\perp}, \tag{B12}$$

$$Q_1 = \left(\frac{s_2 - t_1 - m^2}{s_{12}} \right) \tilde{p}_1 + \frac{t_1}{s_{12}} \tilde{p}_2 + Q_{1\perp}, \tag{B13}$$

$$Q_2 = -\frac{t_2}{s_{12}} \tilde{p}_1 + \left(\frac{m^2 + t_2 - s_1}{s_{12}} \right) \tilde{p}_2 + Q_{2\perp}, \tag{B14}$$

$$Q_3 = \left(\frac{s_2 - m^2 + t_2 - t_1}{s_{12}} \right) \tilde{p}_1 + \left(\frac{s_1 - m^2 + t_1 - t_2}{s_{12}} \right) \tilde{p}_2 + Q_{3\perp}. \tag{B15}$$

The most important assumption of the Reggeon calculus is that the $2 \to 2$ subamplitudes inside the hybrid Feynman graph have Regge behavior in their subenergies for fixed momentum transfer and finite off-shell masses, and that they decrease rapidly for large momentum transfers or masses. These assumptions translate into stringent restrictions on the possible ranges of Sudakov parameters.

First consider the hybrid Feynman graph shown in Fig. 10(a) where the blobs are the $2 \to 2$ subamplitudes which are assumed to have the Regge

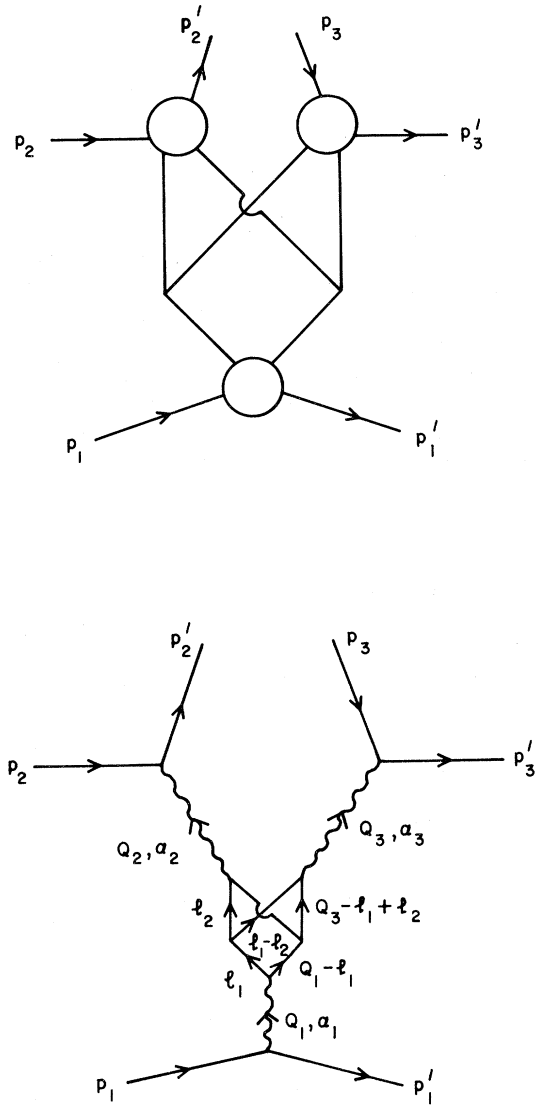

FIG. 10. Triple-Regge pole graph for Appendix B.

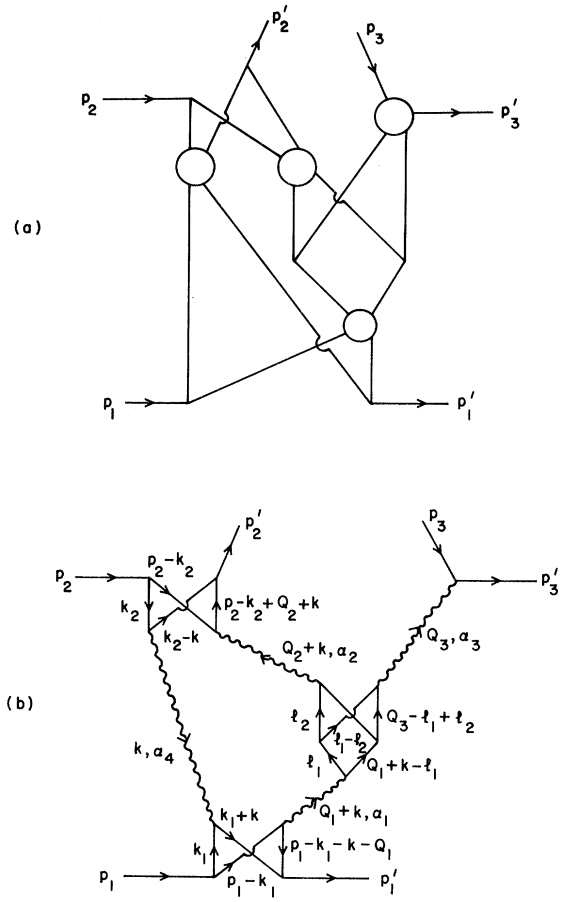

FIG. 11. Regge-cut graph for Appendix B.

behavior as described above. This leads to the graph shown in Fig. 10(b) after this assumption is invoked. Parameterizing the internal momenta l_i as

$$l_i = A_i \tilde{p}_i + B_i \tilde{p}_2 + l_{i_\perp} \tag{B16}$$

and using

$$d^4 l_i = \frac{|s_{12}|}{2} dA_i \, dB_i \, d^2 l_{i_\perp} \tag{B17}$$

allows one to carry out all but the integrals over the transverse plane. This graph leads to the conventional triple-Regge pole graph in the triple-Regge limit and corresponds to the expression

$$T_6(\text{pole}) = -\beta(t_1)\beta(t_2)\beta(t_3) s_{12}^{\alpha_2} \xi_{\alpha_2} s_{13}^{\alpha_3} \xi_{\alpha_3} s_1^{\alpha_1 - \alpha_2 - \alpha_2} \times \xi_{\alpha_1 - \alpha_2 - \alpha_3} r_{\alpha_1, \alpha_2, \alpha_3}, \tag{B18}$$

where the β's are the particle-particle-Reggeon couplings, $r_{\alpha_1, \alpha_2, \alpha_3}$ is the triple-Regge coupling, and ξ_α is the signature factor, defined as

$$\xi_\alpha = \frac{(\tau + e^{-i\pi\alpha})}{-\sin\pi\alpha}. \tag{B19}$$

Next we turn to the analysis of the hybrid Feynman graph shown in Fig. 11(a). It is sufficient to identify various pieces in this graph which one already encounters in the analysis of hybrid graphs for the $2 \to 2$ elastic amplitudes and the triple-Regge pole graph discussed above. The objects of interest are the two-Reggeon two-particle function N and the triple-Reggeon coupling $r_{\alpha_1, \alpha_2, \alpha_3}$ from the analysis of the $2 \to 2$ amplitudes and the triple-Regge pole graph. After replacing all the $2 \to 2$ subamplitudes by their power behavior, i.e., Regge poles, this graph leads to the graph shown in Fig. 11(b) and corresponds

to the expression

$$T_6 = -i \int \frac{d^4k}{(2\pi)^4} g^2 \int \frac{d^4k_1}{(2\pi)^4} \frac{\beta^2}{D_1 \cdots D_4} g^2 \int \frac{d^2k_2}{(2\pi)^4} \frac{\beta^2}{D_5 \cdots D_8} \times g^2 \int \frac{d^4l_1 d^4l_2}{(2\pi)^8} \frac{\beta^3}{D_9 \cdots D_{14}} \xi_{\alpha_1}[(p_1 - k_1 - l_1)^2]^{\alpha_1} \xi_{\alpha_2}[(p_2 + l_2 - k_2)^2]^{\alpha_2} \times \xi_{\alpha_3}[(p_3 + l_2 - P_2)^2]^{\alpha_3} \xi_{\alpha_4}[(k_1 + k_2)^2]^{\alpha_4}, \quad \text{(B20)}$$

where

$$\alpha_1 = \alpha((Q_1 + k)^2), \quad \text{(B21)}$$

$$\alpha_2 = \alpha((Q_2 + k)^2), \quad \text{(B22)}$$

$$\alpha_3 = \alpha(Q_3^2), \quad \text{(B23)}$$

$$\alpha_4 = \alpha(k^2) \quad \text{(B24)}$$

are the Regge trajectories, and the D_i are the denominators from the various particle propagators. Decompose k, k_i, and l_i in terms of the Sudakov parameters as

$$k = a\tilde{p}_1 + b\tilde{p}_2 + k_\perp, \quad \text{(B25)}$$

$$k_i = a_i\tilde{p}_1 + b_i\tilde{p}_2 + k_\perp, \quad i = 1, 2 \quad \text{(B26)}$$

and

$$l_i = A_i\tilde{p}_1 + B_i\tilde{p}_2 + l_{i\perp}, \quad i = 1, 2. \quad \text{(B27)}$$

Next examine each particle propagator D_i and require that it remain finite, i.e.,

$$D_i \lesssim m^2 \text{ for all } i. \quad \text{(B28)}$$

For the lower vertex of Fig. 8(b) this means that

$$k_1^2 = a_1 b_1 s_{12} + k_{i\perp}^2 \lesssim m^2, \quad \text{(B29)}$$

$$(p_1 - k_1)^2 = (1 - a_1) b_1 s_{12} + k_{1\perp}^2 \lesssim m^2, \text{ etc.} \quad \text{(B30)}$$

from which we learn that

$$|b_1| \lesssim \frac{m^2}{s_{12}}, \quad |b| \lesssim \frac{m^2}{s_{12}}, \quad |a_1| \lesssim 1, \quad |a| \lesssim 1, \quad k_{1\perp}^2 \lesssim m^2. \quad \text{(B31)}$$

A similar analysis on the upper left vertex gives

$$|a_2| \lesssim \frac{m^2}{s_{12}}, \quad |a| \lesssim \frac{m^2}{s_{12}}, \quad |b_2| \lesssim 1, \quad |b| \lesssim 1, \quad k_{2\perp}^2 \lesssim m^2, \quad \text{(B32)}$$

and together these require that

$$|a| \lesssim m^2/s_{12}, \quad |b| \lesssim m^2/s_{12}. \quad \text{(B33)}$$

As a next step in the analysis, we require that each Reggeon carry energy $\gg m^2$, which means that

$$\alpha_1: \quad (p_1 - k_1 - l_1)^2 \approx (1 - a_1)(-B_1)s_{12}, \quad \text{(B34)}$$

$$\alpha_2: \quad (p_2 + l_2 - k_2)^2 \approx A_2(1 - b_2)s_{12}, \quad \text{(B35)}$$

$$\alpha_3: \quad (p_3 + l_1 - l_2)^2 \approx (A_1 - A_2)s_{13}, \quad \text{(B36)}$$

$$\alpha_4: \quad (k_1 + k_2)^2 \approx a_1 b_2 s_{12}. \quad \text{(B37)}$$

These equations have incorporated in them the result following from the demand that the particle propagators $D_9 \cdots D_{14}$ in the center be $\lesssim m^2$. The Reggeon energies are large only if

$$\frac{m^2}{s_{12}} \ll |a_1|, |b_2|, |b_1|, |A_2|, \text{ and } |A_1 - A_2|. \quad \text{(B38)}$$

Next one uses these results about the sizes of the parameters a and b in examining the various pieces of the graph shown in Fig. 11(b).

First look at the lower cross: Its denominators are

$$D_1 = k_1^2 - m^2 + i\epsilon = s_{12}a_1b_1 + k_{1\perp}^2 - m^2 + i\epsilon, \quad \text{(B39)}$$

$$D_2 = (p_1 - k_1)^2 - m^2 + i\epsilon = (1 - a_1)\left(\frac{m^2}{s_{12}} - b_1\right)s_{12} + k_{1\perp}^2 - m^2 + i\epsilon, \quad \text{(B40)}$$

$$D_3 = (k_1 + k)^2 - m^2 + i\epsilon = a_1(b_1 + b)s_{12} + (k_1 + k_\perp)^2 - m^2 + i\epsilon, \quad \text{(B41)}$$

$$D_4 = (p_1 - k_1 - k - Q_1)^2 - m^2 + i\epsilon = (1 - a_1)\left(\frac{m^2}{s_{12}} - b_1 - b - \frac{t_1}{s_{12}}\right)s_{12} + (k_1 + k + Q_1)_\perp^2 - m^2 + i\epsilon. \quad \text{(B42)}$$

Note that the parameter a does not appear here since it is much smaller [$O(m^2/s_{12})$] than a_1. Hence the lower vertex has no dependence on a. The same type of analysis shows that the D_i in $(D_5 \cdots D_8)$ have no dependence on b. Furthermore, the central triple-Regge vertex depends on neither a nor b and has precisely the form of $r_{\alpha_1,\alpha_2,\alpha_3}$ which appear in the triple-Regge pole graph.

Collecting together the integration of the central vertex gives

$$\xi_{\alpha_1}\xi_{\alpha_2}\xi_{\alpha_3}s_{12}^{\alpha_1+\alpha_2}s_{13}^{\alpha_3}\frac{g^2|s_{12}|^2}{4(2\pi)^8}\int dA_1 dB_1 d^2l_{1\perp}dA_2dB_2d^2l_{2\perp}\frac{\beta^3}{D_9\cdots D_{14}}(-B_1)^{\alpha_1}A_2^{\alpha_2}(A_1-A_2)^{\alpha_3}$$

$$\equiv -\xi_{\alpha_1}\xi_{\alpha_3}\xi_{\alpha_1-\alpha_2-\alpha_3}s_{12}^{\alpha_2}s_{13}^{\alpha_3}s_1^{\alpha_1-\alpha_2-\alpha_3}\gamma_{\alpha_1,\alpha_2,\alpha_3}. \tag{B43}$$

We move the b integration down to the lower vertex and note that

$$\frac{g^2|s_{12}|}{2(2\pi)^4}\int db\int da_1db_1d^2k_{1\perp}\frac{(1-a_1)^{\alpha_1}a_1^{\alpha_4}\beta^2}{D_1\cdots D_4}=N_{\alpha_1,\alpha_4}\sqrt{2}\,\frac{2\pi}{|s_{12}|}, \tag{B44}$$

where the N_{α_1,α_4} is the same two-Reggeon–two-particle function which appears in the analysis of the elastic amplitude. Similarly, moving the a integration to the upper left vertex gives us N_{α_2,α_4}. Collecting the various pieces together we find that the final expression which corresponds to the Feynman amplitude for Fig. 11(b) is

$$T_6=\tfrac{1}{4}i\int\frac{d^2k_\perp}{(2\pi)^2}N_{\alpha_1\alpha_4}N_{\alpha_2\alpha_4}\gamma_{\alpha_1,\alpha_2,\alpha_3}s_{12}^{\alpha_2+\alpha_4-1}s_{13}^{\alpha_3}s_1^{\alpha_1-\alpha_2-\alpha_3}\xi_{\alpha_2}\xi_{\alpha_3}\xi_{\alpha_4}(\xi_{\alpha_1-\alpha_2-\alpha_3}). \tag{B45}$$

The invariant cross section is given by

$$s\frac{d\sigma}{dt\,dM^2}=\sigma=\frac{1}{2i}\,\mathrm{Disc}_{s_1=M^2}T_6(s_{12}=s+i\epsilon,\ s_{13}=s-i\epsilon,\ s_1=M^2,\ t_1=0,\ t_2=t_3=t). \tag{B46}$$

Taking the Mueller discontinuity of Eq. (B45) eliminates the $\xi_{\alpha_1-\alpha_2-\alpha_3}$ and replaces the ξ_{α_3} with $\xi^*_{\alpha_3}$ but does not change any of the vertices. Thus if we make the replacements

$$\alpha_1\to\alpha_3,\quad \alpha_2\to\alpha_2,\quad \alpha_3\to\alpha_1,\quad \alpha_4\to\alpha_4,$$
$$s_{12}\to s,\quad s_{13}\to s,\quad s_1\to M^2, \tag{B47}$$

then upon taking the discontinuity we obtain Eq. (3.1).

APPENDIX C: ABSORPTION MODEL FOR $N_{\alpha_2\lambda_c;\alpha_1\lambda_a}$

In this appendix we derive Eq. (3.21), the absorption model for the Reggeon-particle vertex $N_{\alpha_2\lambda_c;\alpha_1\lambda_a}$. By definition this is given by a product of Regge residues for the two Reggeons, so we must study the φ' dependence of a product of two S-matrix elements:

$$N_{\alpha_2\lambda_c;\,\alpha_1\lambda_a}\propto\sum_{\lambda'}\langle\theta,0,\lambda_c|S|\theta',\varphi',\lambda'\rangle\times\langle\theta',\varphi',\lambda'|S|0,0,\lambda_a\rangle. \tag{C1}$$

Recall from Jacob and Wick[21] that

$$\langle\theta,\varphi,\lambda_1,\lambda_2|S|\theta',\varphi',\lambda_1',\lambda_2'\rangle=\sum_{J\,M}\frac{2J+1}{4\pi}D^J_{M\lambda}(R(\varphi,\theta,-\varphi))^*\times D^J_{M\lambda'}(R(\varphi',\theta',-\varphi'))\times\langle\lambda_1,\lambda_2|S^J|\lambda_1',\lambda_2'\rangle,\quad \lambda=\lambda_1-\lambda_2,\quad \lambda'=\lambda_1'-\lambda_2', \tag{C2}$$

where as usual

$$R(\alpha,\beta,\gamma)=e^{-i\alpha J_z}e^{-i\beta J_y}e^{-i\gamma J_z},$$
$$D^J_{m\,m'}(R(\alpha,\beta,\gamma))=e^{-im\alpha}d^J_{m\,m'}(\beta)e^{-im'\gamma}. \tag{C3}$$

Using the "particle-one" convention for λ_a, λ_c, and λ', we then find that

$$\langle\theta',\varphi',\lambda'|S|0,0,\lambda_a\rangle=\sum_J\frac{2J+1}{4\pi}D^J_{\lambda_a\lambda'}(R(\varphi',\theta',-\varphi'))^*\times\langle\lambda'|S^J|\lambda_a\rangle, \tag{C4}$$

$$\langle\theta,0,\lambda_c|S|\theta',\varphi',\lambda'\rangle=\sum_J\frac{2J+1}{4\pi}D^J_{\lambda_c\lambda'}(R(\varphi'',\theta'',-\psi''))\times\langle\lambda_c|S^J|\lambda'\rangle,$$

where

$$R(\varphi'', \theta'' - \psi'') = R^{-1}(0, \theta, 0)R(\varphi', \theta', -\varphi'). \quad \text{(C5)}$$

By explicit calculation this gives

$$\cos\theta'' = \cos\theta\cos\theta' + \sin\theta\sin\theta'\cos\varphi', \quad \text{(C6a)}$$

$$\tan\tfrac{1}{2}(\varphi'' - \psi'') = -\frac{\sin\frac{1}{2}\theta\sin\frac{1}{2}\theta'\sin\varphi'}{\cos\frac{1}{2}\theta\cos\frac{1}{2}\theta' + \sin\frac{1}{2}\theta\sin\frac{1}{2}\theta'\cos\varphi'}, \quad \text{(C6b)}$$

$$\tan\tfrac{1}{2}(\varphi'' + \psi'') = \frac{\cos\frac{1}{2}\theta\sin\frac{1}{2}\theta'\sin\varphi'}{-\sin\frac{1}{2}\theta\cos\frac{1}{2}\theta' + \cos\frac{1}{2}\theta\sin\frac{1}{2}\theta'\cos\varphi'}. \quad \text{(C6c)}$$

From Eq. (C3) and Eq. (C4),

$$\langle \theta', \varphi', \lambda' | s | 0, 0, \lambda \rangle = e^{-i(\lambda' - \lambda_a)\varphi'} f_{\lambda'\lambda_a}(\theta'), \quad \text{(C7a)}$$

$$\langle \theta, 0, \lambda_c | s | \theta', \varphi', \lambda' \rangle = e^{-i\lambda_c\varphi'' + i\lambda'\psi''} \times (-1)^{\lambda_c - \lambda'} f_{\lambda_c\lambda'}(\theta''), \quad \text{(C7b)}$$

where

$$f_{\lambda\mu}(\theta) = \sum_J \frac{2J+1}{4\pi} d^J_{\mu\lambda}(\theta)\langle \lambda | s^J | \mu \rangle. \quad \text{(C8)}$$

We now apply these results to the Reggeon-particle vertex. Since Eq. (C6a) is the usual formula for the scattering angle at the second vertex, the Reggeon α_2 is guaranteed to have the correct momentum transfer t''. For large s and small t, t', and t'' we have $\sin\frac{1}{2}\theta \approx 0$, $\sin\frac{1}{2}\theta' \approx 0$, so from Eq. (C6b) and (C6c)

$$\psi'' \approx \varphi'' \approx \tan^{-1}\frac{\cos\frac{1}{2}\theta\sin\frac{1}{2}\theta'\sin\varphi'}{-\sin\frac{1}{2}\theta\cos\frac{1}{2}\theta' + \cos\frac{1}{2}\theta\sin\frac{1}{2}\theta'\cos\varphi'}. \quad \text{(C9)}$$

Then from Eq. (C7) and the definition of the Reggeon-particle vertex we obtain

$$N_{\alpha_2\lambda_c;\,\alpha_1\lambda_a} = \sum_{\lambda'} (-1)^{\lambda_c - \lambda'} e^{-i(\lambda_c - \lambda')\varphi''} \beta^{\alpha_2}_{\lambda_c\lambda'}(t'') \times e^{-i(\lambda' - \lambda_a)\varphi'} \beta^{\alpha_1}_{\lambda'\lambda_a}(t'), \quad \text{(C10)}$$

which is the desired result.

---

*Work supported, in part, by Energy Research and Development Administration.

†On leave from Brookhaven National Laboratory.

[1]R. D. Field and G. C. Fox, Nucl. Phys. B80, 367 (1974).
[2]R. D. Field, in BNL Workshop on Physics with Polarized Targets, 1974 (unpublished).
[3]H. D. I. Abarbanel and D. J. Gross, Phys. Rev. Lett. 26, 732 (1971).
[4]G. R. Goldstein and J. F. Owens, Tufts Univ. report, 1975 (unpublished).
[5]K. Ahmed, J. G. Korner, and G. Kramer, DESY Report No. 75/39 (unpublished).
[6]J. Randa and A. Donnachie, Nucl. Phys. B109, 495 (1976).
[7]T. L. Trueman, in BNL Workshop on Physics with Polarized Targets, 1974 (unpublished).
[8]A. H. Mueller, Phys. Rev. D 2, 2963 (1970).
[9]H. D. I. Abarbanel, G. F. Chew, M. L. Goldberger, and L. M. Saunders, Phys. Rev. Lett. 26, 937 (1971).
[10]A. Pignotti and L. Caneschi, Phys. Rev. Lett. 22, 1219 (1969).
[11]I. J. Muzinich, F. E. Paige, T. L. Trueman, and L. L. Wang, Phys. Rev. D 6, 1048 (1972).
[12]For a review of two-body Regge phenomenology, see G. C. Fox and C. Quigg, Annu. Rev. Nucl. Sci. 23, 219 (1973).
[13]F. E. Paige and D. P. Sidhu, Phys. Rev. D 13, 3015 (1976).
[14]C.-I Tan, Phys. Rev. D 4, 2412 (1971).
[15]H. P. Stapp, Phys. Rev. D 3, 3177 (1971).
[16]H. Pilkuhn *et al.*, Nucl. Phys. B65, 460 (1973).
[17]H. D. I. Abarbanel, J. B. Bronzan, J. Bartels, and D. P. Sidhu, Phys. Rev. D 12, 2459 (1975).
[18]F. E. Paige and T. L. Trueman, Phys. Rev. D 12, 2422 (1975).
[19]V. N. Gribov, Zh. Eksp. Teor. Fiz. 53, 654 (1967) [Sov. Phys.—JETP 26, 414 (1968)].
[20]V. N. Gribov and A. A. Migdal, Yad. Fiz. 8, 1002 (1968) [Sov. J. Nucl. Phys. 8, 583 (1969)]; 8, 1128 (1968) [8, 703 (1969)].
[21]M. Jacob and G. C. Wick, Ann. Phys. (N.Y.) 7, 404 (1959).
[22]The t variables defined here become equal to those in Eq. (3.2) as $s \to \infty$.
[23]L. Dick *et al.*, Phys. Lett. 57B, 93 (1975).
[24]G. Giacomelli, Phys. Rep. 23C, No. 2 (1976).
[25]We use Solution I of Ref. 1.
[26]P. H. Stuntebeck *et al.*, Phys. Rev. D 9, 608 (1973).
[27]A. Borg *et al.*, Nuovo Cimento 22A, 559 (1974).
[28]E. Arik and G. Engels (private communication).
[29]K. Jaeger *et al.*, Phys. Rev. D 11, 2405 (1975).
[30]G. Bunce *et al.*, Phys. Rev. Lett. 36, 1113 (1976).